



Review

Polysaccharides as Economic and Sustainable Raw Materials for the Preparation of Adsorbents for Water Treatment

Gema Díaz Bukvic ^{1,2} , Ezequiel Rossi ^{1,2} and María Inés Errea ^{1,2,*}

¹ Instituto Tecnológico de Buenos Aires (ITBA), Lavardén 315, Ciudad Autónoma de Buenos Aires C1437FBG, Argentina; gediaz@itba.edu.ar (G.D.B.); ezrossi@itba.edu.ar (E.R.)

² Consejo Nacional de Investigaciones Científicas y Técnicas (CONICET) Godoy Cruz 2290, Ciudad Autónoma de Buenos Aires C1425FQB, Argentina

* Correspondence: merrea@itba.edu.ar

Abstract: Adsorption processes, due to their technical simplicity and cost-effectiveness, have arisen as one of the most well-known, straightforward solutions to water pollution. In this context, polysaccharides, due to their abundance, biodegradability, and biocompatibility, are appealing raw materials for the design of adsorbents. Moreover, some of them, such as chitosan, can be obtained from organic waste products, and their use additionally contributes to solving another concerning problem: organic waste accumulation. Unfortunately, due to their low adsorption capacities and/or physicochemical properties, native polysaccharides are not suitable for this purpose. However, there are alternatives that can overcome these physical or chemical limitations, often taking advantage of the versatility of their polyhydroxylated structure. In this context, this review aims to present an overview of the advances from 2019 onwards in the design of new adsorbents for water treatment from cellulose, alginate, chitosan, and starch, addressing the two main strategies reported in the literature: the preparation of either polysaccharide-based composites or polysaccharide derivatives. It is important to point out that, herein, special emphasis is placed on the relationship between the chemical structure and the efficiency as adsorbents of the analyzed materials, in an attempt to contribute to the rational design of adsorbents obtained from polysaccharides.

Keywords: adsorption; polysaccharides' chemical modification; water pollutants; water treatment



Citation: Díaz Bukvic, G.; Rossi, E.; Errea, M.I. Polysaccharides as Economic and Sustainable Raw Materials for the Preparation of Adsorbents for Water Treatment. *Polysaccharides* **2023**, *4*, 219–255. <https://doi.org/10.3390/polysaccharides4030016>

Academic Editor: Priyanka Sharma

Received: 3 July 2023

Revised: 8 August 2023

Accepted: 16 August 2023

Published: 20 August 2023



Copyright: © 2023 by the authors. Licensee MDPI, Basel, Switzerland. This article is an open access article distributed under the terms and conditions of the Creative Commons Attribution (CC BY) license (<https://creativecommons.org/licenses/by/4.0/>).

1. Introduction

Water is a scarce natural resource globally, not only due to its limited physical access but also to the progressive deterioration in its quality caused by pollution [1]. Over the last century, freshwater use has increased by a factor of six and has been growing at a rate of one per cent per year since 1980, which is a result of population growth, economic development, and consumption habits. Some concerning facts reported by the United Nations are that eight out of ten people lack drinking water access in rural areas, and by 2030, only 81% of the need for clean water will be met, which means that 1.6 billion people would not manage to have safe water by then [2]. Thus, one of the greatest challenges of the XXI century is guaranteeing access to safe drinking water. Hence, technologies aiming to pursue this goal intend to make water affordable and accessible for all by developing efficient systems for polluted water remediation [3,4].

Depending on the target pollutant and its concentration, contaminated water can be treated via biological, physical, and chemical processes. These approaches include several technologies such as aeration [5], filtration [6–8], flotation [9–11], coagulation [12–14], flocculation [15], skimming [16,17], chlorination [18,19], membrane technologies [20–22], ozonation [23], oxidation and advanced oxidation processes [24,25], neutralization [26], and adsorption [27–29], among others.

Moreover, adsorption processes have famously provoked interest among the scientific community since they provide a simple, feasible, cost-effective, and straightforward solution to water pollution [30,31].

Adsorption is a superficial phenomenon in which one or more fluid phase components interact with a solid surface, adhering to it. Based on interaction forces between the adsorbate (the substance attached to the surface) and the adsorbent (which provides the surface where adsorbate adheres), adsorption can be either physical (physisorption) or chemical (chemisorption) [32].

One of the main differences between physisorption and chemisorption lies in enthalpy values of 40 kJ mol^{-1} or lower for physical adsorption and higher values for chemically governed adsorption processes [33,34]. Adsorbents' capacity, selectivity, and adsorption rate is determined by their structure and properties [34–39]. It is therefore crucial to study the materials to select the most adequate material according to the pollutants found.

There is a wide variety of adsorbents, which include conventional materials such as inorganic materials (e.g., zeolites, aluminas, silica gel, iron oxides, and clays), activated carbons, ion-exchange resins; and non-conventional adsorbents such as polysaccharides and their derivatives (e.g., chitosan, cellulose, starch, alginate, or cyclodextrin), biosorbents (e.g., algae, fungi, or yeasts) and either by-products or waste from agricultural and industrial activities (e.g., sawdust, corn cob, sugar bagasse, wheat straw, or sewage sludges) [40].

In this context, polysaccharides are materials that are remarkable for their low cost and environmentally friendliness. Unfortunately, as it will be discussed throughout this manuscript, due to either their low adsorption capacities, physicochemical properties or both, polysaccharides are not suitable for water treatment in their native form. However, their polyhydroxylated structure provides them enough versatility to be subjected to chemical modifications in order to impart specific physicochemical properties depending on the products' final application.

Taking into account the above discussion, this review aims to present an overview of the advances from 2019 onwards in the design of new adsorbents suitable for water treatment, made from cellulose, alginate, chitosan, and starch, addressing the two main strategies reported in literature: the preparation of either polysaccharide-based composites or polysaccharide derivatives. Moreover, it is important to point out that, herein, special emphasis is placed on the relationship between the chemical structure and the efficiency as adsorbents of the analyzed materials, in an attempt to contribute to the rational design of adsorbents from polysaccharides.

2. Polysaccharides Involved in Water Remediation

Among naturally existing polysaccharides, cellulose, alginate, chitosan, and starch are the most studied in this field because of their remarkable relative abundance and availability.

2.1. Cellulose

It is well known that cellulose, one of the most abundant organic compounds on Earth, is composed of D-glucopyranose units linked by β -(1→4) bonds (Figure 1).

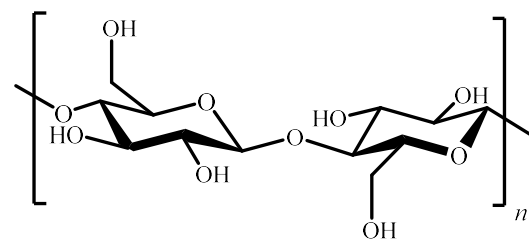


Figure 1. Chemical structure of cellulose.

Although traditionally cellulose has been mainly obtained from wood, over the past few decades, alternative vegetable sources have been increasingly researched to relieve

the demand on wood-based biomass and improve process sustainability [41]. In this context, grasses such as bamboo as well as agricultural residues and agro-industrial crop by-products are among the most explored sources due to their low initial cost and fast regeneration. In the case of waste, their use also contributes to their valorisation [41], but they have as a drawback a lower content of cellulose than wood due to the higher content of lignin and hemicellulose [42].

The search for alternatives beyond vegetable sources has led to the study of bacterial cellulose. Bacterial cellulose is produced via fermentation with specific bacteria under suitable conditions and is obtained as a highly hydrated gelatinous pellicle that grows on the aerated surface of the fermentation vessel [43]. Bacterial cellulose is recognized for its high crystallinity, polymerization degree, and chemical purity, as well as for its unique intrinsic nanofibrillar structure. Furthermore, while the isolation of cellulose from plant sources implies the use of reagents that can have a negative environmental impact, bacterial cellulose is produced free of lignin, hemicelluloses, and pectin, thus, avoiding the need for aggressive chemical treatments for the removal of these compounds [38].

The production of bacterial cellulose has the disadvantage of being more expensive than plant cellulose since until now, it has mainly been produced using specific bacteria, typically *Komagataeibacter xylinus* (formerly called *Gluconacetobacter xylinus* and *Acetobacter xylinum*), which require axenic conditions and strict control of fermentation variables [44]. However, for certain applications, it could be alternatively obtained from the floating pellicle developed during kombucha tea production, in a much simpler process which does not require laboratory conditions, complex growth media, or sophisticated cultivation and processing equipment [44,45]. Given the proliferation in recent years of not only classical home-scale breweries, but also larger-scale kombucha enterprises, this production method offers an attractive alternative to obtain pure cellulose by valorising this by-product of kombucha tea.

As far as cellulose tridimensional structure is concerned, the D-glucopyranose units of its chains have a linear arrangement that allows for the formation of numerous intercatenary hydrogen bonds, which result in the polymer's water insolubility [46] (Figure 2). Additionally, this cellulose arrangement is responsible for its low surface area and consequent low adsorption efficiency of pollutants when employed unmodified, necessitating the functionalization of cellulose [47,48].

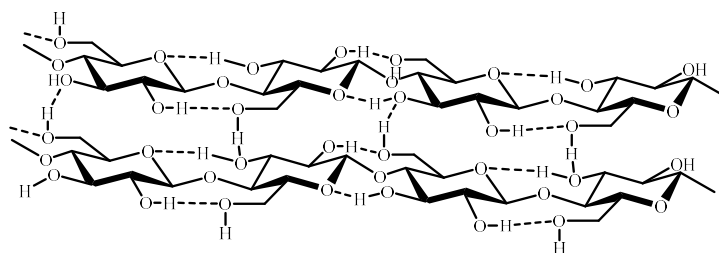


Figure 2. Rearrangement of cellulose chains.

In fact, He et al. illustrated the enhanced adsorption capacity when native cellulose was modified. In this case, native cellulose achieved maximum capacity values of 9.8 and 14.3 mg g⁻¹ for Cr (III) and Fe (III), while 377.2 and 84.0 mg g⁻¹ were attained by preparing a porous spherical polyethyleneimine-cellulose (PEI-cell) absorbent [49].

In that context, intensive work has been carried out on the design of efficient adsorbents from cellulose. The strategies are based either on the preparation of composite materials or on chemical modifications to this polymer.

Approaches to composite materials reported in literature include the preparation of cellulose-based materials using alginate [50–54], chitosan [55–59], hydroxyapatite [60–62], crown ethers [63], graphene oxide (GO) [64,65], magnetite (Fe₃O₄) [66,67], montmorillonite [68–73], titanium dioxide [74], collagen [75], bentonite [76,77], and activated carbon [78,79], among others. Some of them are shown in the table below (Table 1).

Table 1. Adsorption studies carried out over cellulose composite materials (N/R: not reported).

Composite Material	Adsorbate	Optimum pH	Isotherm Model	Kinetic Model	Maximum Adsorption Capacity (mg g ⁻¹)	Reference
Cellulose-based modified citrus peels/calcium alginate composite	Methylene blue (MB) Crystal violet	6.5	Langmuir	Pseudo-second order	923.1 882.0	[50]
Nanocrystalline cellulose/sodium alginate/K-carrageenan composite hydrogel	Pb (II)	N/R	Langmuir	Pseudo-second order	351.0	[51]
Glutaraldehyde crosslinked calcium alginate/cellulose bead	Pb (II)	5.0	Freundlich	Pseudo-second order	206.8	[52]
Calcium alginate hydrogels reinforced with cellulose nanocrystals	MB	7.0	Langmuir	Pseudo-first order	676.7	[53]
Coffee ground cellulose/sodium alginate double-network hydrogel beads	MB Congo red (CR)	N/R	Langmuir-Freundlich	Pseudo-second order	400.5 411.5	[54]
Chitosan/cellulose nanofibril composite membrane	MB	7.0	Langmuir	Pseudo-first order	14.7	[55]
Zeolitic imidazolate framework-67 modified bacterial cellulose/chitosan composite aerogel	Cu (II) Cr (VI)	6.0	N/R	Pseudo-second order	200.6 152.1	[56]
Cellulose/chitosan composite aerogel	CR	7.0	Langmuir	Pseudo-second order	381.7	[57]
Ethylenediamine-modified nanofibrillated cellulose/chitosan composites	MB	4.0	N/R	N/R	19.5	[58]
	New Coccine	2.0			96.7	
Cellulose microfibril-grafted-hydroxyapatite	Pb (II) Cu (II)	N/R	Langmuir	Pseudo-second order	143.8 83.1	[60]
Cellulose-graft-polyacrylamide/hydroxyapatite composite hydrogel	Cu (II)	7.0	N/R	Pseudo-second order	175.0	[61]
Cellulose/hydroxyapatite nanocomposites	Chlortetracycline hydrochloride	7.0	Freundlich	Pseudo-second order	139.4	[62]
Supramolecular polysaccharide composite materials from cellulose, chitosan, and crown ether	Cd (II)	6.0	N/R	Pseudo-second order	49.1	[63]
	Zn (II)				15.2	
	2,4,5-trichlorophenol				6.4	
Graphene oxide incorporated into cellulose acetate beads	MB	7.0	Langmuir	Pseudo-second order	369.9	[64]

Table 1. Cont.

Composite Material	Adsorbate	Optimum pH	Isotherm Model	Kinetic Model	Maximum Adsorption Capacity (mg g ⁻¹)	Reference
Crystalline nanocellulose anchored to reduced graphene oxide	Aspirin Acetaminophen	4.0	N/R	Pseudo-second order	99.0 76.3	[65]
Acrylic acid grafting and amino-functionalized magnetized TEMPO-oxidized cellulose nanofiber	Pb (II)	5.3	Freundlich	Pseudo-second order	122.0	[66]
Microcrystalline cellulose/Fe ₃ O ₄ composite	Malachite green	7.0	Freundlich	Pseudo-second order	2.9	[67]
Cellulose/montmorillonite mesoporous composite beads	Auramine O dye	7.0	Redlich-Peterson	Pseudo-second order	1336.2	[68]
Directional cellulose nanofiber/chitosan/montmorillonite aerogel	Cu (II) Pb (II) Cd (II)	2.0	Langmuir	Pseudo-second order	181.9 170.2 163.9	[69]
Crosslinked cellulose nanofibrils/alkali lignin/montmorillonite/polyvinyl alcohol network hydrogel	MB	10.5	N/R	Pseudo-second order	67.2	[70]
Bamboo nanocellulose/montmorillonite nanosheet/polyethyleneimine gel adsorbent	MB Cu (II)	10.0 5.0	Sips	Fractal-like pseudo-second order	361.9 254.6	[71]
Na-montmorillonite/cellulose nanocomposite	Cr (VI)	4.0	Langmuir	Second order	22.3	[72]
Electrospun composite nanofiber mats of cellulose/organically modified montmorillonite	Cr (VI)	3.0	N/R	N/R	18.5	[73]
Titanium oxide-bacterial cellulose bioadsorbent	Pb (II)	7.0	N/R	N/R	200.0	[74]
Waste collagen, polyethyleneimine, and carbon dots cross-linked by aldehyde cellulose nanofibers	Cr (VI)	2.0	Langmuir	Pseudo-second order	103.3	[75]
Cellulose/bentonite-zeolite composite	Brilliant green	5.6	Langmuir	Pseudo-second order	99.1	[76]
Microcrystalline cellulose/bentonite-grafted polyacrylic acid hydrogel	Cd (II)	6.0	Freundlich	Pseudo-second order	242.5	[77]
3D porous structured cellulose nanofibril-based hydrogel with carbon dots	Cr (VI)	2.0	Langmuir	Pseudo-second order	116.0	[78]
Activated carbon/carborundum/microcrystalline cellulose core shell nano-composite	As (III) Cu (II)	6.0	Freundlich	Pseudo-second order	422.9 423.6	[79]

Nonetheless, in most of the mentioned cases, the main role of cellulose was just to provide mechanical resistance, a porous matrix insoluble in water, or both, while the metal adsorption capacity was provided by the other materials chosen for the adsorbents' preparation.

Regarding chemical modifications of cellulose, strategies are based on the chemical reactivity of the hydroxyl groups. These reactions are intended to confer cellulose-specific features according to the target pollutant and can be divided into two groups:

- i. Polymerization in the presence of adequate monomers (grafting).
- ii. Reactions of the hydroxyl groups with compounds possessing the functionalization needed according to the final application.

Among the different monomers grafted onto cellulose aiming to enhance its adsorption capacity, acrylic acid [80–83], acrylamide [84], methacrylic acid [85], acrylonitrile [86–88], vinyl acetate [89], and 2-hydroxyethyl methacrylate [90] can be mentioned. In all cases, after grafting the monomers onto cellulose, grafted polymers can be subjected to crosslinking reactions or subsequent modifications [91].

In the case of hydroxyl groups' chemical modifications, some only aim to disrupt hydrogen bonds interactions to increase the exposure of the internal chains' hydroxyl groups to the adsorbates. An example of such modifications is the preparation of cellulose crosslinked with crown ethers, such as dibenzo-18-crown 6, using ceric ammonium nitrate as the initiator, which was found to be suitable for Cd (II), Zn (II), Ni (II), Pb(II) and Cu(II) as described by A. Fakhre et al. [92]. Moreover, the crown ether-immobilized cellulose acetate membranes presented by Oana Steluta Serbanescu et al. were efficient in Gd (III) retention [93]. Other modifications include cellulose subdued to esterification and oxidation processes for Cu(II) removal as described by Dutta Gupta et al., using octenyl succinic anhydride and sodium hypochlorite, respectively [94].

Other experiments aim to improve cellulose adsorption of ionic pollutants by introducing charged groups into the cellulose's structure. Cationic and anionic exchangers were produced by introducing carboxyl or amino groups, respectively. Furthermore, the preparation of amphoteric materials was also studied.

Among cationic exchangers, carboxylic groups are mainly introduced in cellulose via carboxymethylation (Figure 3). For instance, the preparation of carboxymethyl cellulose (CMC) with the highest substitution degree that still guarantees its water insolubility was reported in [38,95].

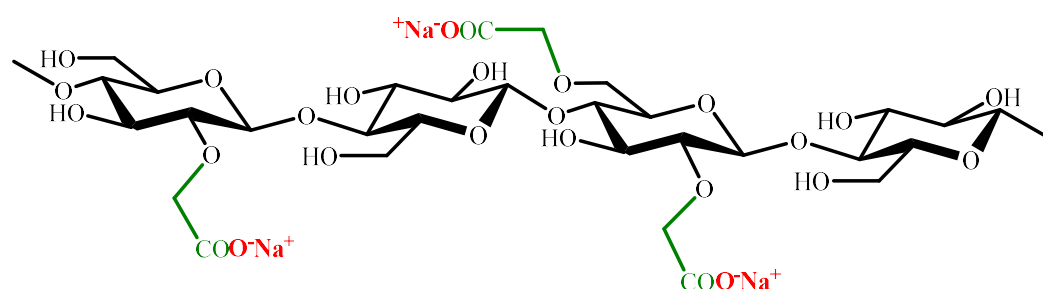


Figure 3. Chemical structure of carboxymethylcellulose.

Further modifications of CMC have led to the production of hydrogels by crosslinking CMC with epichloridrine [96], polyacrylamide [97], and polyvinyl alcohol [98]. Furthermore, Lin et al. carried out a systematic study to obtain cellulose sponges from CMC via treatment of the cellulose derivative with different concentrations of sulphuric acid and a further freeze–thawing treatment, without the need for an organic crosslinker [99].

Over the above-mentioned cellulose derivatives, adsorption studies have been carried out with Pb (II), Cd (II), Cu (II), Ag (I), Hg (II), and Ni (II), and results showed a wide range of adsorption capacity values (Table 2).

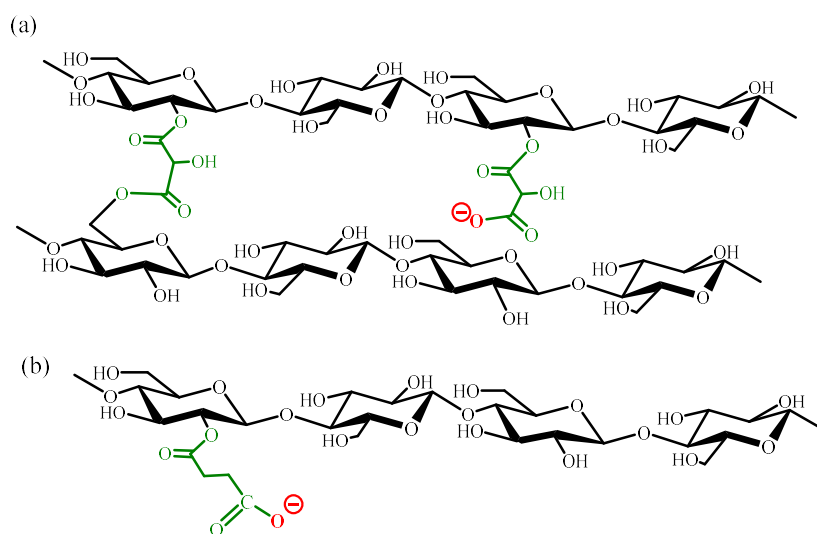
Table 2. Adsorption studies carried out over carboxymethylated cellulose *.

CMC Substitution Degree (Carboxymethyl Groups/Anhydroglucose Units)	Modification	Adsorbate	pH	Isotherm Model	Kinetic Model	Maximum Adsorption Capacity (mg g ⁻¹)	Reference
0.17	None	Pb (II)	7.0	Langmuir	Pseudo-second order	59.5	[38]
0.35	None	Pb (II)	7.0	Langmuir	Pseudo-second order	127.0	[95]
0.65–0.85	Crosslinking in presence of epichloridrine	Cd (II)	6.0	Langmuir	Both pseudo-first and pseudo-second order	~150.0	[96]
N/R	Crosslinking in presence of polyacrylamide	Pb (II)	5.0	Langmuir	Pseudo-second order	~850.0	[97]
N/R	Crosslinking in presence of PVA	Cu (II) Cd (II) Ni (II) Hg (II)	5.0	N/R	N/R	~2.3 ~0.3 ~0.3 ~0.1	[98]
0.7	Crosslinking by heating in presence of sulphuric acid and a further freeze-thawing treatment	Ag (I) Cu (II) Ni (II)	6.6 5.5 6.4	N/R	N/R	7.7 6.8 7.2	[99]

* In all cases the best results obtained are shown.

Regarding the material obtained by Chen et al., not only was it the one with the highest lead adsorption capacity value, but it also exhibited a remarkable adsorption capacity towards the cationic dye MB (1611.4 mg g⁻¹) [97].

In addition to carboxymethylation, other sources of carboxylic groups used to obtain cation exchangers found in the literature include the incorporation of succinic or citric acid via ester bonds into cellulose chains (Figure 4).

**Figure 4.** Modification of cellulose with (a) citric acid; (b) succinic acid.

In the case of succinic derivatives, the one obtained by Gurgel et al. [100] achieved maximum capacity values of 185.2, 256.4, and 500.0 mg g⁻¹ for Cu(II), Cd(II) and Pb(II), respectively. On the other hand, Olivito et al. reported the introduction of citric acid into cellulose structure, observing some measure of crosslinking [101]. This adsorbent was efficient for MB removal, obtaining a maximum capacity value of 96.2 mg g⁻¹. Another cellulose citrate, reported by Tursi et al., exhibited a high affinity and a remarkable maximum adsorption uptake for Hg(II) (1600.0 mg g⁻¹) [102].

On the other hand, the production of anion exchangers can be achieved by introducing amino groups into the cellulose structure, as mentioned above. Under acidic conditions, the amino groups are easily protonated, increasing the affinity of these derivatives to anionic pollutants via electrostatic interactions, compared to native cellulose [103].

In this context, Chen et al. reported on a hyperbranched polyethyleneimine cellulose derivative (Figure 5I) with a high maximum adsorption capacity value for reactive yellow X-RG dye (970.9 mg g⁻¹) [104].

Jin et al. also reported on the preparation of an amino-functionalized nanocrystalline cellulose as an adsorbent for anionic dyes [105]. This work describes the partial oxidative rupture of the cellulose glucopyranose units that led to the formation of aldehyde groups, which were further converted into amino groups via amination-reductive reactions (Figure 5II). The product described by Jin et al. was assayed as adsorbent for the removal of anionic dyes and showed the maximum adsorption capacity value for acid red (555.6 mg g⁻¹).

Moreover, anion exchanger cellulose hydrogels were prepared by modifying cellulose with 2,3-epoxypropyl trimethyl ammonium chloride and crosslinked with poly(ethylene glycol) diglycidyl ether (Figure 5III). The maximum adsorption capacity values of the samples for anionic dyes were found to be between 240.0 and 447.0 mg g⁻¹ [106].

Anirudhan et al. reported a cellulose-based anion exchanger synthesized by a graft polymerization reaction between cellulose and glycidyl methacrylate using *N,N*-methylenebis-acrylamide as a crosslinker, followed by amination with dimethylamine (Figure 5IV) [107]. The authors studied the effectiveness of the exchanger for As(V) removal, reporting a maximum adsorption capacity value of 200.3 mg g⁻¹.

Pereira et al. described an adsorbent for As(V) and Cu(II) removal, prepared by tosylation of microcrystalline cellulose and further nucleophilic substitution of the tosyl group with ethylenediamine (Figure 5V) [108], achieving maximum adsorption capacity values of 121.4 and 69.2 mg g⁻¹, respectively.

Moreover, in recent years, the number of published articles reporting cellulose-based ionic liquid as ionic adsorbents for water treatment has increased significantly. For instance, Dong et al. reported the production of imidazolium-based ionic liquid glycidyl methacrylate grafted cellulose microspheres using 1-aminopropyl-3-methyl imidazolium salts as ionic liquids, with a high adsorption capacity value of 735.3 mg g⁻¹ for Au(III) [109]. Guo et al. also reported gold recovery via another cellulose-based ionic liquid. In their study, carboxymethyl-diethylammoniummethyl cellulose was prepared, but the resulting material had remarkably poor adsorption properties, with maximum capacity value of 15 mg g⁻¹ for Au(III) [110].

Zhang et al. reported the use of cellulose nanocrystals grafted with poly(ionic liquid) prepared via gamma-ray-initiated polymerization of cellulose. The material was assayed via CR and yielded a higher capacity value for the modified composite (195.8 mg g⁻¹), compared to the 59.7 mg g⁻¹ removed using cellulose unmodified nanocrystals [111].

In particular, a highly effective novel magnetic cellulose-based ionic liquid was described by Ling et al. as functionalized by Fe₃O₄ nanoparticles grafted with imidazole ionic liquid followed by the formation of cellulose microspheres modified by polyethyleneimine. The material was efficient for CR and MB, obtaining maximum capacity values of 1299.3 and 1068.1 mg g⁻¹, respectively [112]. Likewise, as reported by Li et al., a functionalized magnetic cellulose was prepared by dissolving microcrystalline cellulose in an ionic liquid, which was further modified with glutaric anhydride [113]. In this case, the adsorbent

achieved maximum adsorption capacity values of 1186.8 and 151.8 mg g⁻¹ for MB and Rhodamine B, respectively. In both cases, in addition to their reusability, the fact that adsorbents possess magnetic properties allows them to be separated from aqueous solutions via the use of an external magnetic field, which is an interesting advantage for green wastewater treatment.

Wan et al. modified cellulose with ionic liquid 4-methylimidazole, obtaining 3D porous microspheres with large surface areas [114], achieving a maximum adsorption capacity value of 218.6 mg g⁻¹ for Acid Orange 7 dye.

Zhang et al. prepared a cellulose-base adsorbent via modification with imidazolium ionic liquid, which was assayed for the removal of other anionic dyes. In this work, the maximum adsorption capacity values obtained were 1169.0 and 563.0 mg g⁻¹ for xylenol orange and CR, respectively. In this case, these adsorption capacity values were 3.5 times higher than those obtained with native cellulose [115].

On the other hand, there are also reports of amphoteric adsorbents obtained from cellulose. For instance, Zhou et al. reported the preparation of a material with a high density of amino and carboxyl groups from microcrystalline cellulose for the simultaneous removal of anionic and cationic heavy metal ions. Herein, the complete removal of Cr (VI), Cd (II), Cu (II), Zn (II), and Pb (II) from an aqueous solution was reported [116].

Zhong et al. synthesized an adsorbent from wheat straw, first introducing quaternary amine groups onto cellulose by reaction with epichlorohydrin, ethylenediamide, and triethylamine. Then, carboxylic groups were introduced via reaction with sodium hydroxide and monochloroacetic acid. Hence, the maximum adsorption capacity values obtained for Cu (II) and Cr (VI) removal with unmodified wheat (16.0 and 30.9 mg g⁻¹, respectively) and the modified amphoteric adsorbent (90.9 and 270.1 mg g⁻¹, respectively) were compared [117].

Kono reported on cellulose polyampholyte hydrogels prepared with a cationization reaction of sodium carboxymethylcellulose with 2,3-epoxypropyltrimethylammonium chloride, crosslinked with ethyleneglycoldiglycidylether. The adsorbent was assayed with Acid Red 9, Acid Red 13, and Acid Blue 92 dyes, obtaining maximum adsorption capacity values of 866, 911, and 816 mg g⁻¹, respectively [118].

In addition, a several-times reusable amphoteric adsorbent was prepared by Zhu et al. from cellulose-grafted calcium hydroxide and assayed for CR and MB dyes. The respective maximum adsorption capacity values were 2552.7 and 756.5 mg g⁻¹ [119].

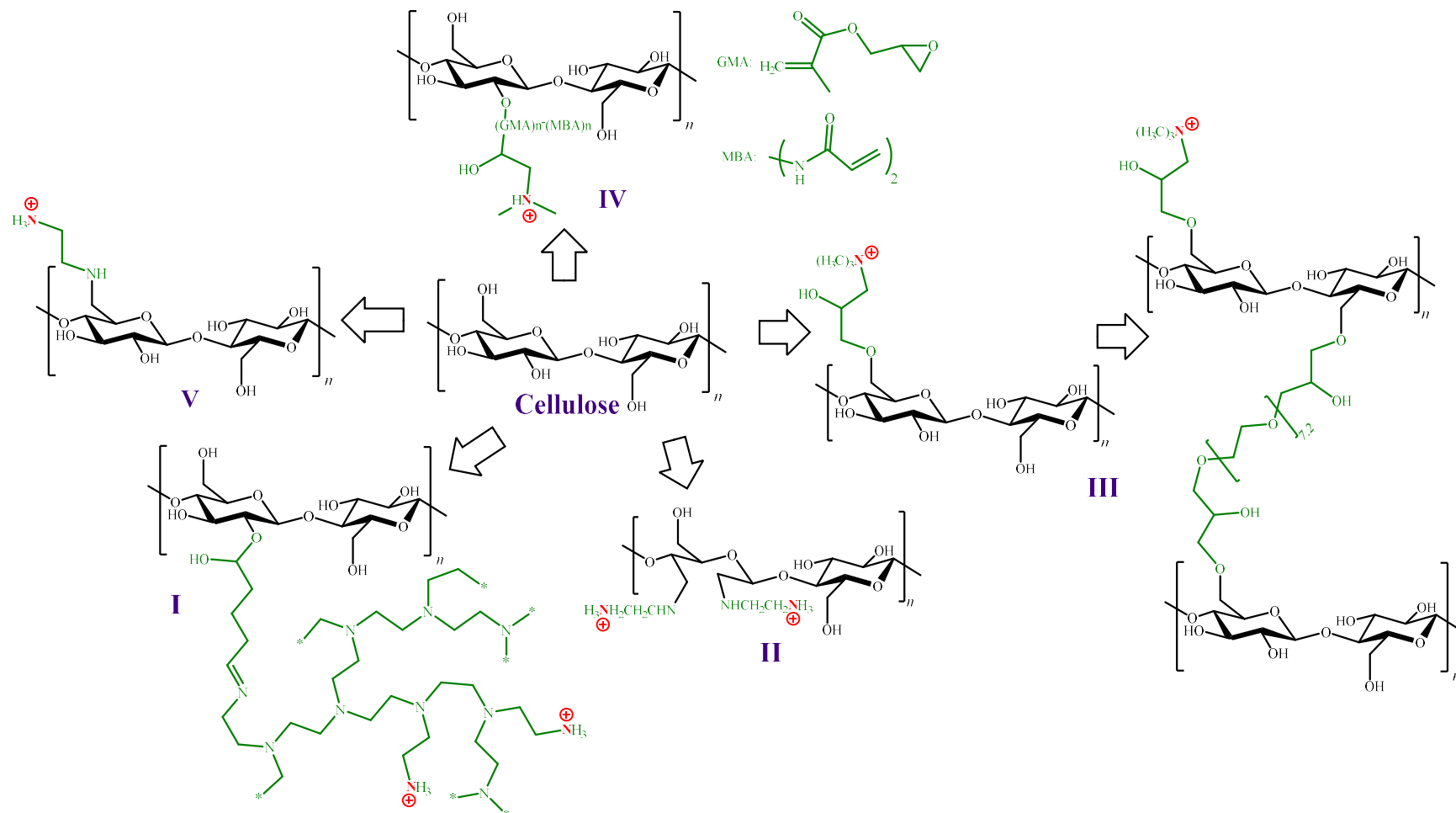


Figure 5. Chemical structures of anion exchangers derived from cellulose.

2.2. Alginate

Alginate is a polysaccharide which naturally exists as its sodium salt and is constituted of (1→4)-linked β -D-mannuronate (M) and α -L-guluronate (G) residues (Figure 6). Alginate does not have regular repetitive units, since it is a block copolymer composed of homopolymeric regions of M or G and interspersed with regions with MG blocks [120].

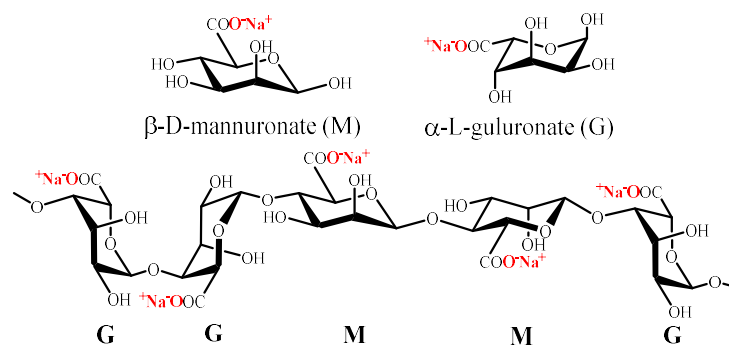


Figure 6. Chemical structure of mannuronate (M), guluronate (G) and alginate.

Its abundance is mainly due to its presence in marine brown algae *Phaeophyceae*, *Ascophyllum nodosum*, *Laminaria hyperborea*, and *Macrocystis pyrifera* as a structure-forming component and in soil bacteria as a capsular polysaccharide. Several bacteria can produce alginate, such as *Azotobacter* sp. and *Pseudomonas* sp. However, commercial alginates are mainly obtained from algal sources, since industrial bacterial production is not economically feasible at present despite being technically possible [121].

The distribution and sequence of M and G blocks of alginate varies according to its source and affects the polysaccharides' properties, such as viscosity. In fact, for example, alginate obtained from brown algae of the specie *Sargassum* is considered to be of "borderline" quality due to its low G content [122]. It is important to note that both the environmental conditions during the growth of algae and the extraction techniques used are also two variables that have a high impact on the final structure of the alginate [123].

The interaction between sodium alginate and divalent or trivalent metal cations produces ionic gelation [124], which is related to the length of G blocks in alginate. The formation of coordinate sites is generated by G chains looping, known as the egg-box model (Figure 7).

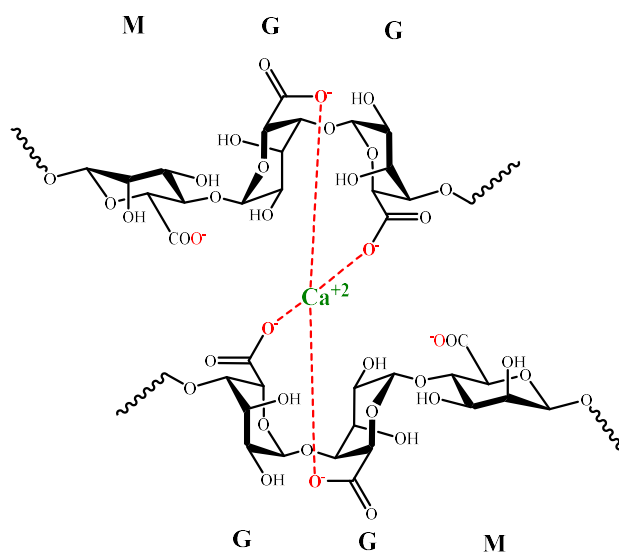


Figure 7. Egg-box model for G alginate residues and $\text{Ca}(\text{II})$.

In the presence of monovalent metal cations such as sodium, alginate acts as semiflexible chains instead of the stiff aggregated rigid chains obtained via egg-box formation with Ca (II) [125].

Calcium alginate beads are well known for their ability to adsorb cationic pollutants. In particular, there is some evidence that relates metal cation size to the adsorption efficacy of alginate beads. Both He et al. and Papageorgiou et al. observed higher adsorption capacity values when cation size increases: Pb (II) > Cu (II) > Cd (II), suggesting that larger ions fit better in binding sites [126,127].

Alginate capsules have been proven to have a high lead-binding capacity, with maximum adsorption capacity values of 1540.0 mg g⁻¹ reported by Gyu Park et al. In this case, capsules were prepared by dropping CaCl₂ solution and xanthan gum into sodium alginate [128].

Vijaya et al. also obtained insoluble calcium alginate beads which were assayed for Ni (II) adsorption, obtaining 310.4 mg g⁻¹ for calcium alginate. Ni (II) uptake was attributed to both pore volume and large surface area [129].

Nevertheless, the mentioned alginate adsorbents still face two main drawbacks: alginate calcium complex instability and low porosity. Additionally, many of the alginate beads tried in packed column operation exhibited pressure drops that were too high to flow and were not rigid enough. Therefore, intensive work has been done to improve their adsorption performance. To this end, Jeon et al. reported an alginic acid immobilized with PVA-boric acid and crosslinked with glutaraldehyde, designed to reduce the hydration of the bead, obtaining a mechanically strong adsorbent, stable at pH levels under 1.0 and temperatures above 170 °C, with a maximum adsorption capacity value of 390 mg g⁻¹ for Pb (II) [130].

Considering the issues mentioned before, another alternative to the use of calcium alginate on its own is the preparation of composite materials as reported in the literature. Some examples are described next.

Wang et al. obtained satisfactory results for heavy metal removal with granular alginate-based hydrogels, prepared via grafting and crosslinking reactions between sodium alginate, acrylic acid, polyvinylpyrrolidone, and gelatine. The maximum adsorption capacity values obtained for Ni (II), Cu (II), Zn (II) and Cd (II) were: 177.7, 199.9, 190.4 and 321.7, mg g⁻¹, respectively. Competitive studies suggested that Cu (II) has a stronger affinity for the hydrogel [131].

Mahji et al. reported the preparation of a polyaniline/sodium alginate composite for the removal of both cationic and anionic dyes. In particular, the adsorption of MB, rhodamine B, orange II, and methyl orange was assessed, reporting maximum adsorption capacity values of 555.5, 434.8, 476.2, and 416.7 mg g⁻¹, respectively [132].

Pashaei-Fakhri et al. were able to graft polyacrylamide onto alginate chains with free radical polymerization, obtaining a hydrogel whose adsorption affinity towards the cationic dye crystal violet was compared with an acrylamide/GO bonded sodium alginate, also prepared by these authors [133]. Results showed that increasing the amount of GO improved the efficiency of the hydrogel in removing the dye studied, but a GO concentration above 5 wt.%, began to decrease in efficiency. This was attributed to the reduction of dye penetration into the hydrogel as a consequence of the agglomeration of the GO nanoparticles [134].

Jiang et al. also reported on the preparation of a sodium alginate-grafted polyacrylamide/GO hydrogel produced via free radical polymerization. In this case, adsorption of Cu (II) and Pb (II) was studied, and maximum adsorption capacity values of 68.8 and 240.7 mg g⁻¹, respectively, were obtained. It is important to highlight that the concentration of GO in the hydrogel was not informed by the authors and, considering the results of Pashaei-Fakhri [133], this data would have been extremely relevant for result comparison.

Zhang et al. prepared alginate-based hydrogels by incorporating polyaniline-polypyrrole-modified GO as reinforced fillers into the alginate matrix [135]. In this paper, the authors reported a GO concentration of 0.5 % w/v. The materials were assayed for the removal of

cationic and anionic heavy metals, achieving maximum adsorption capacity values of 87.2 and 133.7 mg g⁻¹ for Cu (II) and Cr (VI), respectively.

Majdoub et al. also used GO to improve the adsorption capacity of alginate towards cationic heavy metals [136]. In this case, the carboxyl and epoxy groups of GO were used to covalently bond hexamethylenediamine (HDMA) to the GO's surface (GO-HDMA). Further, GO-HDMA was encapsulated in alginate hydrogel beads with different loading (5, 10, 15, and 20 wt.%) yielding alginate/GO-HDMA hybrid adsorbents. Adsorption studies towards Pb (II), Cu (II), and Cd (II) showed almost complete removal of these metals even when a complex matrix, such as tap water was assayed.

Moreover, a modification including both the incorporation of sulphur atoms and GO into the alginate structure was described by Zhang et al., who reported the synthesis of a biocomposite hydrogel in which L-cysteine-modified alginate (TA) was combined with GO for the removal of heavy metal ions from water (Figure 8). TA/GO hydrogel microspheres were prepared by dropping GO, dispersed in water, into a TA water solution. The mixture was then dropped into a CaCl₂ solution, leading to the formation of TA/GO microspheres. TA/GO was assessed as adsorbent towards Pb (II) and Cu (II), and the calculated maximum adsorption capacity values were 369.6 and 124.1 mg g⁻¹, respectively [137].

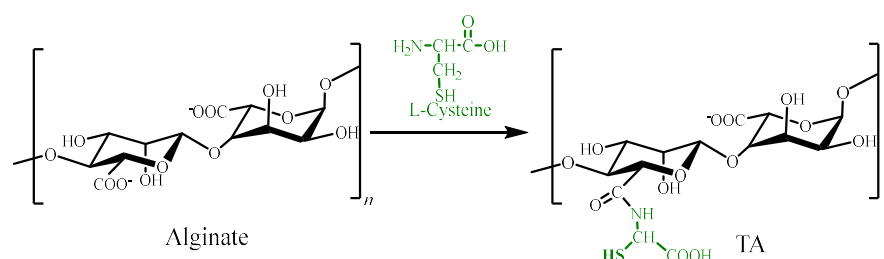


Figure 8. Alginate chemical modification described by Zhang et al. [137].

On the other hand, aerogels have emerged as remarkable adsorbent materials in water treatment for its beneficial characteristics such as adjustable surface chemistry, low density, high specific surface area, and highly porous three-dimensional structure [138–141].

In this context, there is a report of a three-dimensional sodium alginate/gelatine/GO triple network composite aerogel with a 3 wt.% of GO incorporated into its structure. This material was assayed as adsorbent of both anionic and cationic dyes, such as CR and MB [142], with maximum adsorption capacity values of 196.8 and 322.6 mg g⁻¹, respectively.

Wang et al. described the preparation of a calcium alginate disodium ethylenediaminetetraacetate dihydrate hybrid aerogel (aerogel-EDTA) for the removal of heavy metals from wastewater. Results showed high affinity of the adsorbent for Pb (II), Cd (II), Cu (II), Cr (III), and Co (II), exhibiting the highest selectivity towards Cd (II) with a maximum adsorption capacity value of 177.3 mg g⁻¹ [143].

As far as adsorbents with magnetic properties are concerned, a new alginate derivative capable of removing heavy metal ions from an aqueous multicomponent solution containing Pb (II), Cu (II), Cd (II), and Ni (II) was reported [144]. Intrinsically mesoporous halloysite (HNTs) nanoclays, β-cyclodextrin (β-CD), and iron nanoparticles were incorporated into the alginate beads. HNTs, due to their ordered tubular and nano-sized structure, enhance the thermal and chemical stability of the adsorbent [145]. β-CD is a cyclic non-toxic oligosaccharide whose ability to form metal ion complexes is well known [146]. Moreover, the iron nanoparticles confer magnetic properties to the material. Unfortunately, adsorption studies of the alginate derivative showed low maximum adsorption capacity values of 21.1, 15.5, 2.5, and 2.7 mg g⁻¹ for Pb (II), Cu (II), Cd (II), and Ni (II), respectively.

Another magnetic alginate-based composite was described by Alver et al. In this case, a magnetic alginate/rice husk composite was prepared via the ionotropic gelation method [147]. Magnetic properties were achieved by incorporating FeCl₂ into the algi-

nate/rice husk beads. Adsorption studies were carried out towards MB, and results showed a maximum adsorption capacity value of 274.9 mg g^{-1} [148].

Moreover, it is well known that clay minerals and their modified derivatives have high efficacy in removing most of the common chemical contaminants from aqueous solutions. Shi et al. reported hydrazide-modified sodium alginate as an efficient adsorbent of heavy metals [149]. In this case, alginate chains were crosslinked using adipic acid hydrazid as a crosslinker (Figure 9). The ability of the new material to remove Hg (II), Pb (II), Cd (II), and Cu (II) was assayed, yielding maximum adsorption capacity values of 7.8, 2.0, 4.8, and 3.9 mg g^{-1} , respectively.

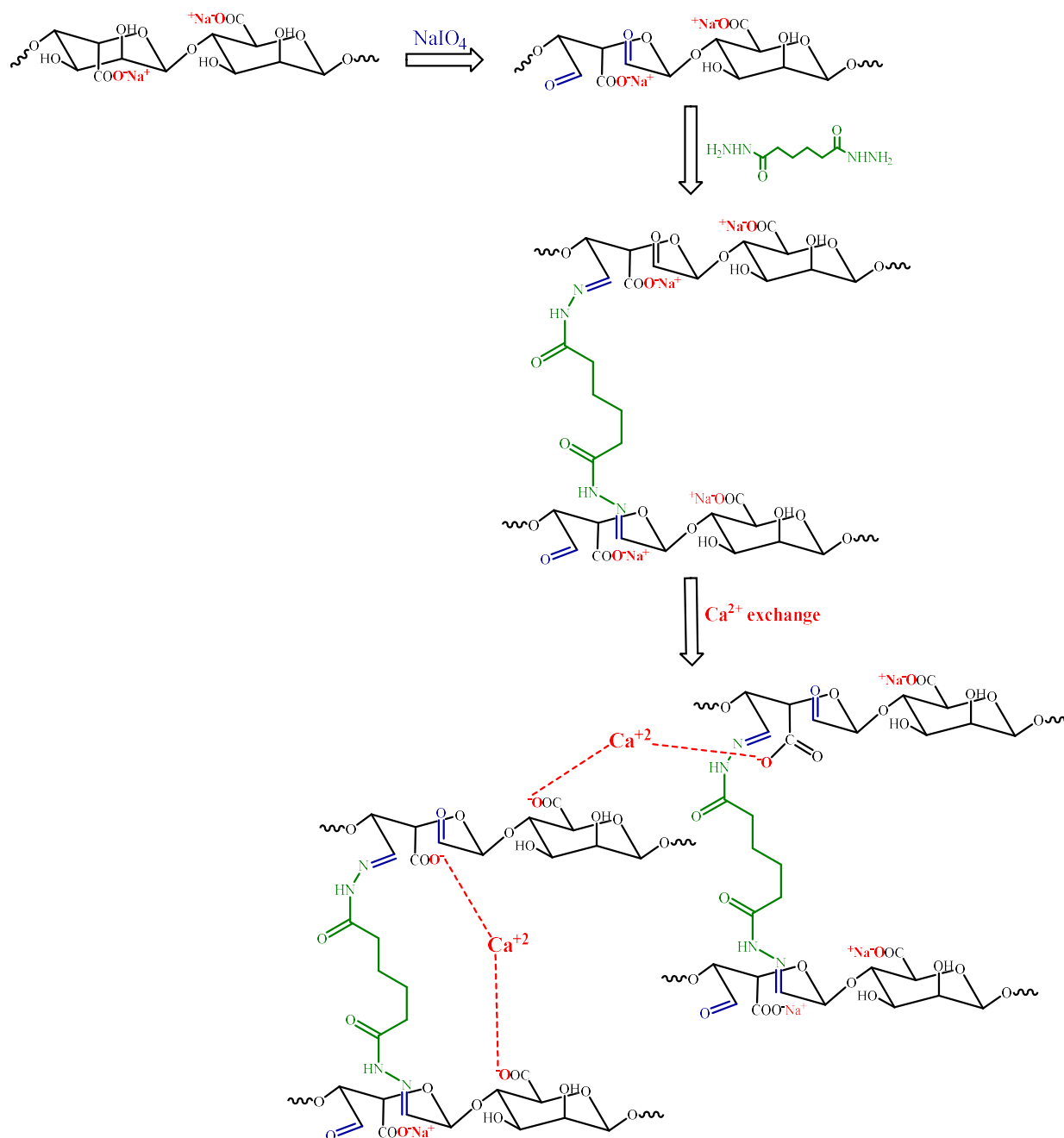


Figure 9. Alginate chemical modifications described by Shi et al. [149].

Among this family of adsorbents, those based on montmorillonite, a typical 2:1 type clay mineral, have been the most extensively studied [150]. Thus, the inclusion of this mineral in an alginate composite is expected to enhance the adsorption capacity of the polysaccharide. In fact, Wang et al. reported the synthesis of a porous montmorillonite nanosheet/poly (acrylamide-co-acrylic acid)/sodium alginate hydrogel beads which could reach a maximum adsorption MB capacity of 530.7 mg g^{-1} [151].

The maximum adsorption capacity for MB reported by Wang was similar to the ones obtained from other alginate composite materials also containing montmorillonite, as stated by Sezen et al. [152].

The use of alginate-based composite materials that include minerals with the aim of enhancing their efficiency for water treatment is also exemplified by the work of Isawi, who reported on the preparation of zeolite/polyvinyl alcohol/sodium alginate nanocomposite beads for the removal of heavy metals from wastewater [153]. The maximum adsorption capacity of this new material at the optimal pH (6) for Pb (II), Cd (II), Sr (II), Cu (II), Zn (II), Ni (II), and Mn (II) were 47.6, 46.3, 47.2, 48.5, 48.3, 47.6 and 46.3 mg g^{-1} , respectively.

Moreover, there is also a report in which waste, in this case, sugar bagasse [154], was chemically modified via ester bonds with succinic acid, leading to sugar bagasse succinate (SBS), which was further used to make an alginate composite material. The new SBS/alginate composite yielded maximum adsorption capacity values of 176.4 and 354.6 mg g^{-1} for Cd (II) and Pb (II), respectively [155].

Furthermore, there are reports of alginate/chitosan composites that are described in the following section.

2.3. Chitosan

Chitosan is a polysaccharide obtained via partial deacetylation of naturally existing chitin, the second most abundant polysaccharide on Earth after cellulose, which can be found in the shells of insects and crustaceans [156,157]. Industrialization and commercialization of shrimps and prawns are relevant to the economy of many countries but, at the same time, crustacean shells accumulate when discarded, with a significant negative environmental impact. Therefore, the utilization of this waste contributes to solving environmental problems associated with its accumulation [37,158].

Chemical structure of chitosan (poly (β (1 \rightarrow 4)-2-amino-2-deoxy-D-glucopyranose) is shown in Figure 10 [159].

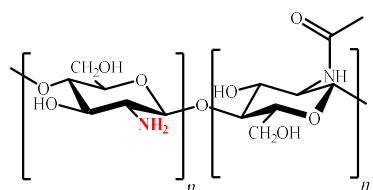


Figure 10. Chemical structure of partially acetylated chitosan.

Considering that the amino groups of the D-glucosamine residues of chitosan (Figure 9) have a pKa value of 6.5 [34], at pH values below 6.5 they are predominantly positively charged, making chitosan a polycation [37]. Nevertheless, despite the polycation's capacity to form ionic complexes with a wide variety of anionic pollutants [160], its complete solubility in aqueous media at pH values lower than 5 limits its use as adsorbent [34,37].

On the other hand, regarding cationic pollutants such as lead, mercury, copper, cobalt, and cadmium, among others, chitosan chains must be predominantly deprotonated to avoid electrostatic repulsion and, therefore, pH values above 6.5 are required. In this case, the main mechanism involved in metal retention is chelation, in which the amino groups play a key role, serving as coordination sites for metal-binding [160,161]. Additionally, it is important to highlight that cation diffusion into chitosan's structure could affect its adsorption capacity, depending on the physical nature of chitosan (i.e., flakes, beads, or membranes) and its crystallinity [160,161].

From an economic point of view, the use of an adsorbent on an industrial scale is only feasible if it is reusable, so regeneration of the materials is critical. Hence, the fact that chitosan is soluble in the acidic aqueous mediums required for heavy metal desorption prevents it from regenerating and consequently from being used on a large scale.

Therefore, efforts are focused towards producing insoluble chitosan materials in an acidic environment and enhancing the materials' adsorption capacity. In this context, the main strategies reported include: substitutions involving either the C-6 hydroxyl group, the C-2 amino group, or both; crosslinking reactions; and grafting of polymeric chains.

For instance, Zhao et al. reported an amphoteric crosslinked chitosan with citric acid esterified β -cyclodextrin (Figure 11) [162]. The material was reported as effective for the removal of many common dyes, including reactive blue 49, reactive yellow 176, reactive blue 14, reactive black 5, and reactive red 141, which vary in size and structure, showing the versatility of the materials for pollutant removal. The authors used reactive blue 49 as the model adsorbate, and under the optimum adsorption conditions, up to 500 mg g^{-1} was adsorbed.

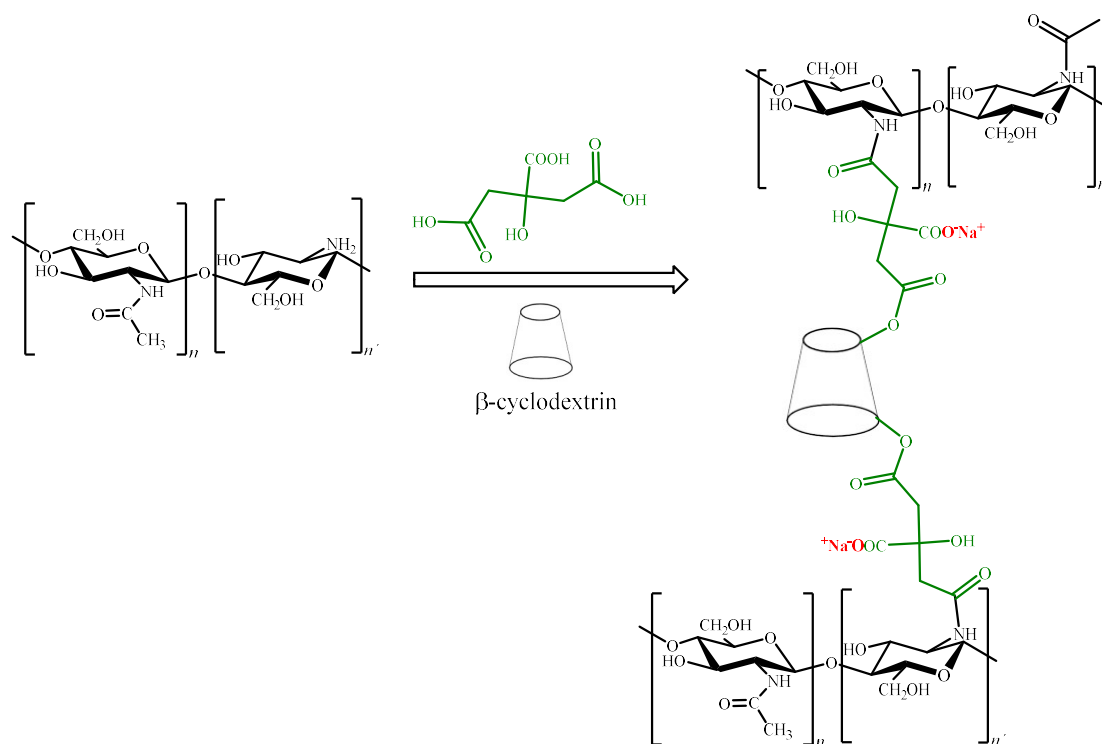


Figure 11. Chitosan-modified chemical structure reported by Zhao et al. [162].

A synthetic strategy similar to the one employed by Zhao [162] was carried out by Usman et al. [163], who also used a β -cyclodextrin as a modifying chitosan agent to prepare an adsorbent for dye removal from wastewater. In this case, nitrilotriacetic acid was used instead of citric acid and glutaraldehyde was chosen as a crosslinker. The maximum MB adsorption capacity of the material was 162.6 mg g^{-1} , which is lower than that reported by Zhao.

Karimi-Maleh et al. reported the preparation of 1-butyl-3-methylimidazolium bromide impregnated chitosan beads and the product was assayed as adsorbent for the removal of the cationic dye MB [164]. However, a maximum adsorption capacity value of just 7 mg g^{-1} was reported.

Fan et al. reported the synthesis of a CO_2 -responsive chitosan aerogel, and the results achieved for adsorption and desorption of Cu (II) were reported. The authors synthesized a polyacrylic acid 2-(dimethylamino)ethyl methacrylate (P(AA-co-DMAEMA)), which was combined with chitosan via physical crosslinking via electrostatic interactions between

the carboxyl and amino groups in chitosan. Then, porous chitosan/P(AA-co-DMAEMA) aerogels (CPA) were obtained by freeze-drying. The calculated Cu (II) maximum adsorption capacity value of the material was 163.7 mg g^{-1} . In this work the most remarkable feature was that the heavy metal could be desorbed by CO_2 bubbling under mild conditions, avoiding the use of strong acids usually involved in metal desorption processes. The desorption rate reported by the authors surpassed 80%. It is important to note that after 6 cycles, the adsorption capacity of CPA for Cu (II) still reached 70% of the initial adsorption capacity [165].

There are also reports of lignosulphonate/chitosan adsorbents for the removal of heavy metals from wastewater [166,167]. Lignins are important resources found in large amounts as waste products in paper industry effluents. They are highly branched phenolic polymers with a vast number of aromatic monomers derived from three monolignols (*p*-coumaryl, coniferyl and sinapyl alcohols; Figure 12) [168–170].

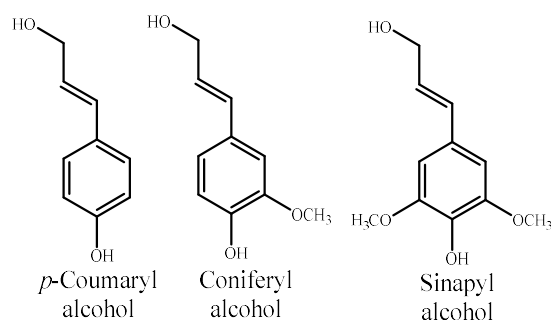


Figure 12. Lignin precursors (monolignols).

Within this kind of chitosan-based material, Mu et al. reported a free radical polymerization method for the synthesis of a porous lignosulphonate/chitosan material, which was assayed as adsorbent towards Co (II) and Cu (II), finding maximum adsorption capacity values of 386.0 and 283.0 mg g^{-1} , respectively. In the case of Zhang et al., the chitosan derivative was obtained in a similar way to the one reported by Mu, and the authors reported a high efficiency of this material as a Pb (II) adsorbent (maximum adsorption capacity value: 525.0 mg g^{-1}) [166,167].

Rossi et al. described the preparation and characterization of water insoluble chitosan derivatives using mucic and adipic acid (a polyhydroxylated and a non-functionalized diacid of the same length chain, respectively) as a crosslinkers. In highly regioselective reactions, *N*-substituted crosslinked chitosan derivatives were achieved and their efficiency as lead adsorbent was assessed. Maximum adsorption capacity values of 76.3 and 69.7 mg g^{-1} were reported for chitosan crosslinked with mucic and adipic acid, respectively, evidencing the role of the crosslinker hydroxyl groups in the lead adsorption mechanism on the chitosan derivative [34].

Besides, as stated in the previous Section, there are recent reports of chitosan/alginate composites described as adsorbents of heavy metals or dyes.

For instance, Zhao et al. prepared a fibrous chitosan/sodium alginate composite foam by freeze-drying with ternary acetic acid/water/tetrahydrofuran solvents and compared its maximum adsorption capacity against selected dyes to the ones obtained preparing the same composite but using the classic binary mixture of solvents (acetic acid/water) instead. The hypothesis of the authors was that solvents play a key role in the transformation of the microstructure of the composite into finer scale structure, increasing the adsorption capacity of the material. The composite material prepared with the ternary mixture of solvents showed a significantly higher maximum adsorption capacity values towards the cationic dye MB than the ones observed for the composite obtained using the binary mixture of solvents (1488.1 and 560.2 mg g^{-1} , respectively) [171].

In the case of Tang et al., a physically crosslinked hydrogel of chitosan/sodium alginate/calcium ion was prepared. The adsorbent was assayed as a heavy metals adsorbent.

The maximum adsorption capacity values towards Pb (II), Cu (II) and Cd (II), reached 176.5, 70.8 and 81.2 mg g⁻¹, respectively [172].

Ablouh et al. reported the obtention of chitosan microspheres/sodium alginate hybrid bead for heavy metals removal from aqueous solutions. In this work, maximum adsorption capacity values of 180 and 16 mg g⁻¹ for Pb (II) and Cr (VI), respectively, were achieved. These results clearly show the higher efficiency of this material for the removal of cationic pollutants [173].

Among this kind of composite materials, Khapre et al. proposed a chitosan crosslinked with glutaraldehyde/alginate composite as adsorbent of dyes from water solutions. Adsorption studies towards methyl orange, brilliant green and patent blue V were carried out, achieving between moderate and low maximum adsorption capacity values of 198.1, 235.8, and 117.3 mg g⁻¹, respectively [174].

A similar composite was prepared by Hamza et al. (Figure 13) but, in this case, adsorption of Cd (II) and Pb (II) was assessed [175]. The sorbent was first studied as adsorbent of each heavy metal, obtaining maximum adsorption capacity values of 220.5 and 258.6 mg g⁻¹ for Cd (II) and Pb (II), respectively. Furthermore, the new material was assayed for its use on water samples collected from an industrial area with a high concentration of various heavy metals, showing a drastically decrease in the pollutants' concentration in the effluents.

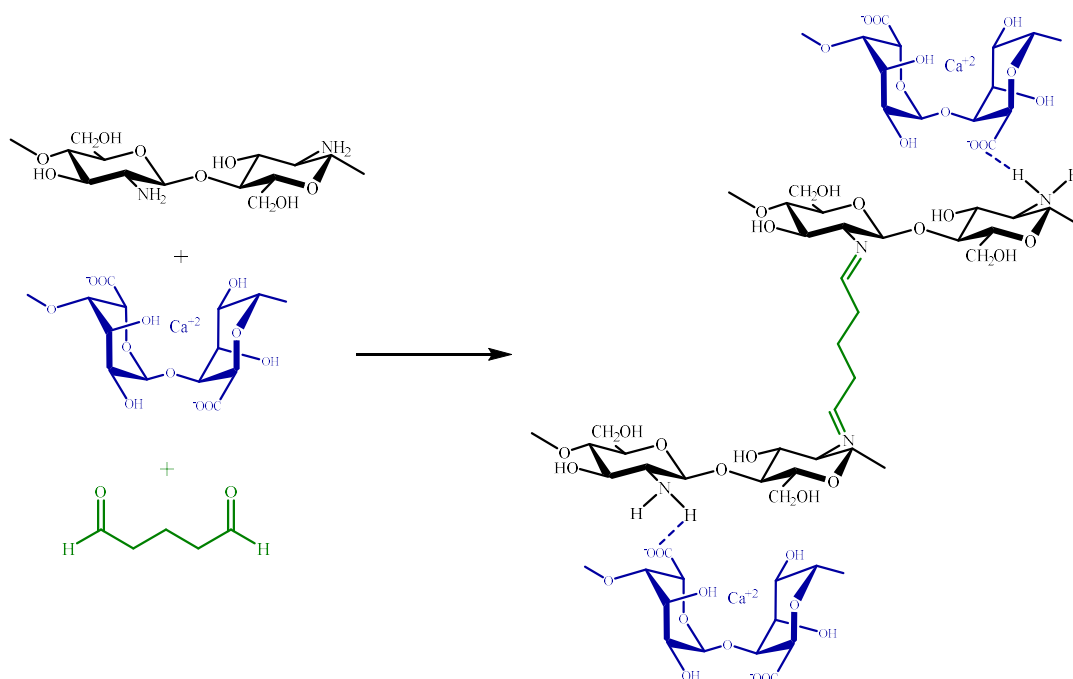


Figure 13. Hydrogel of chitosan/sodium alginate/calcium ion reported by Tang et al. [172].

2.4. Starch

Researchers have been also focused on other abundant polysaccharide: starch. It is constituted by two homopolysaccharides, amylose and amylopectin [176]. The former is a water-soluble linear polymer, consisting in D-glucopyranose units linked by α -(1 \rightarrow 4) bonds. Amylopectin has a branched structure with mostly short chains of α -(1 \rightarrow 4) linked D-glucopyranose units with 5–6% branches linked by α -(1 \rightarrow 6) glycosidic bonds to the main chain (Figure 14) [177].

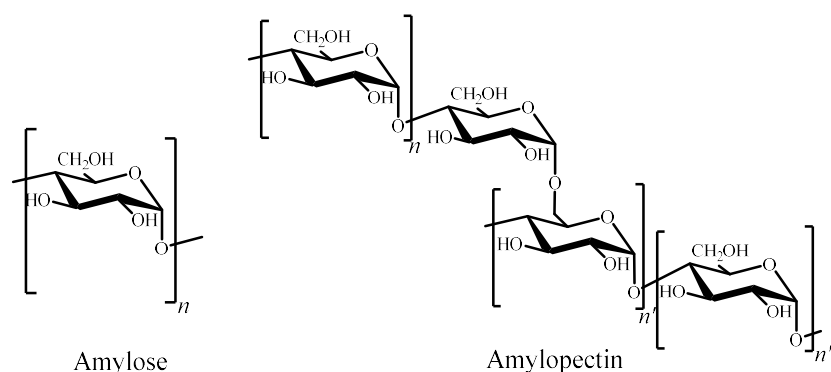


Figure 14. Chemical structures of amylose and amylopectin.

Depending on the source from which starch is obtained, the proportion of amylose and amylopectin varies, and so does its average molecular weight [178]. Some of the most common sources include maize, potato, wheat and rice. Nevertheless, there are promising unconventional sources under study, such as fruits and vegetables waste. Kringel et al. conducted studies on amylose and amylopectin content of waste from fruits and vegetables with the aim of analysing its suitability as valorised residues from natural sources. The reported starch content of outer pericarp and core tissues of kiwi, mango kernels, pineapple stems, apple pulp, banana peels and avocado seeds was in a 20–50% range [179].

Regarding water treatment, native starch has been reported to have a poor adsorption capacity [180], which can mainly be attributed to its low surface area, limited thermal stability and absence of highly-absorptive functional groups, such as carboxyl, xanthate, acrylate, acetyl, hydroxypropyl, amine or amide [181,182]. Analogously to cellulose, alginate and chitosan, there are reports describing starch's chemical modifications as well as the preparation of starch composites.

For instance, Guo et al. compared the efficiency for MB removal attained by native starch and a modified porous derivative, prepared by crosslinking native starch with epichlorohydrin and further hydrolysis with α -amylase, obtaining a maximum adsorption capacity value for MB almost three times higher than native starch [183]. In accordance with the results reported by Guo et al., Alvarado et al. also observed an enhancement of the adsorption capacity for the MB of starch after being modified by esterification with malonic, glutaric and valeric acids [184].

Soto et al. also compared modified and native starch. In this case, maleic acid and itaconic acids were used for esterification of starch, achieving maximum adsorption capacity values for Pb (II) and Zn (II) of 25.2 and 7.9 mg g⁻¹, respectively for itaconate starch, while 5.2 and 3.2 mg g⁻¹ were the corresponding values for native starch [185]. Soto et al. also reported oxidized starch adsorbents that achieved higher heavy metal removal capacity values compared to native starch; for Cd (II): 11.1 and 8.0 mg g⁻¹; for Ni (II): 22.6 and 8.3 mg g⁻¹; for Pb (II): 18.0 and 5.2 mg g⁻¹; and for Zn (II): 10.3 and 3.2 mg g⁻¹, respectively [186].

Sancey et al. reported the crosslinking of starch with 1,4-butanediol diglycidylether in presence of ammonium hydroxide and 2,3-epoxy-propyltrimethylammonium chloride, with further carboxymethylation. Herein, metal adsorption studies were conducted, achieving almost complete removal of Cu (II) and Fe (III) [187]. Copper removal was also assayed by Zheng et al. using starch hydrogels prepared with poly(acrylic acid), achieving an uptake of 179.9 mg g⁻¹ Cu(II) in aqueous medium [188].

Chaudhari et al. prepared a starch xanthate that achieved almost complete removal of Hg (II), Cu (II), Cd (II) and Ni (II), and attributed the heavy metals uptake to the complexation of metals with xanthate groups [189].

As far as starch composites are concerned, composites with layer double hydroxide for methyl orange and fluoride removal from wastewater were reported. These materials were prepared by co-precipitation and different metals were used for the hydroxide layers,

such as Mg (II), Al (III), Zn (II), Fe (III) and Ni (II). In particular, Zubair et al. reported a Starch-Ni/Fe-layered double hydroxide composite that achieved a maximum methyl orange (MO) adsorption capacity value of 387.6 mg g^{-1} [190]. However, Tao et al. achieved a higher maximum adsorption capacity value towards MO of 1555.0 mg g^{-1} [191] for the Zn/Mg/Al-Layered double hydroxide starch. On the other hand, a Mg/Al layered double hydroxides reported by Liu et al. achieved almost complete removal of fluoride [192].

Besides, iron nanoparticles are well-known to contribute to arsenic removal due to electrostatic attraction, ion exchange, and surface complexation [193]. It is therefore interesting to analyze iron nanoparticles' effect when used in materials prepared with starch, such as composite materials with magnetite, maghemite and ferromanganese binary oxide. Next, some of the reported materials are described, in which starch acted only as a support or stabilizer of the mentioned inorganic particles.

Adsorption studies towards As (III) on iron-starch materials were carried out in aqueous solutions, achieving a maximum adsorption capacity value of 161.3 mg g^{-1} with the material reported by Xu et al. [194], while Siddiqui et al., obtained a maximum capacity value of 8.9 mg g^{-1} for a functionalized maghemite [195] and Robinson et al., 55.9 mg g^{-1} for a starch/maghemite nano-adsorbent [196].

On the other hand, as in the case of the other polysaccharides mentioned in previous sections, the preparation of ion exchangers from starch is a widely used strategy for ionic pollutants removal. For instance, Ma et al. [197] chemically modified starch attaching either xanthate or citrate groups to their structure (Figure 15I,II). In this work, adsorption assays towards Pb (II) were carried out, and the maximum adsorption capacity values were 109.1 and 57.6 mg g^{-1} for starch xanthate and starch citrate, respectively.

Another strategy for introducing negative charges in the starch structure is the oxidation of C-6 to a carboxyl group (Figure 15III). In this context, Liu et al. [198] modified starch nanoparticles through oxidization, using sodium hypochlorite. The new materials were preliminarily explored as adsorbents of heavy metals, using Pb (II) and Cu (II) as adsorbate models. Compared to the unmodified nanoparticles, the modified ones had remarkably higher adsorption capacity values (94.5 and 81.0 mg g^{-1} for Pb (II) and Cu (II), respectively).

Chen et al. [199] also used starch nanoparticles, but in this case the incorporation of negative charges in their surface was achieved by esterification with succinyl anhydride (Figure 15IV). The maximum degree of substitution was 0.1, which resulted in an increase on the surface Z-potential. The modified nanoparticles were assayed for the adsorption of Cu (II) and MB, showing that the adsorption process was greatly influenced by the pH value, as expected in presence of carboxyl groups. At low pH values, carboxyl groups are highly protonated, and the adsorption could be neglected (less than 3.0 mg g^{-1}). At pH values above 4.0, the degree of protonation decreases and the surface charge of the adsorbents becomes negative, exerting electrostatic attraction to the adsorbate [34,38], which enhances the adsorption capacity of Cu (II) and MB (8.4 and 24.4 mg g^{-1} , respectively).

Another example of modifications to obtain negatively charged starch was performed by Hashem et al. [200], who reported starch hydrogels prepared via graft polymerization of acrylonitrile, followed by nitrile groups hydrolysis to generate carboxylic acids and amides (Figure 15V). In this work, adsorption of Hg (II) on the starch hydrogels were carried out and a maximum adsorption capacity value of 1250 mg g^{-1} was reported by the authors. Subsequently, the same author reported adsorption studies against Pb (II) carried out on a similar material. In this last case, the value of the maximum adsorption capacity value reported was 264.4 mg g^{-1} [201].

Haroon et al. [202] also obtained cation exchangers by grafting carboxymethylated starch with *N*-vinylpyrrolidone (Figure 15VI). The new material was assayed as adsorbent towards rhodamine 6G from wastewater with a maximum adsorption capacity value of 363.9 mg g^{-1} .

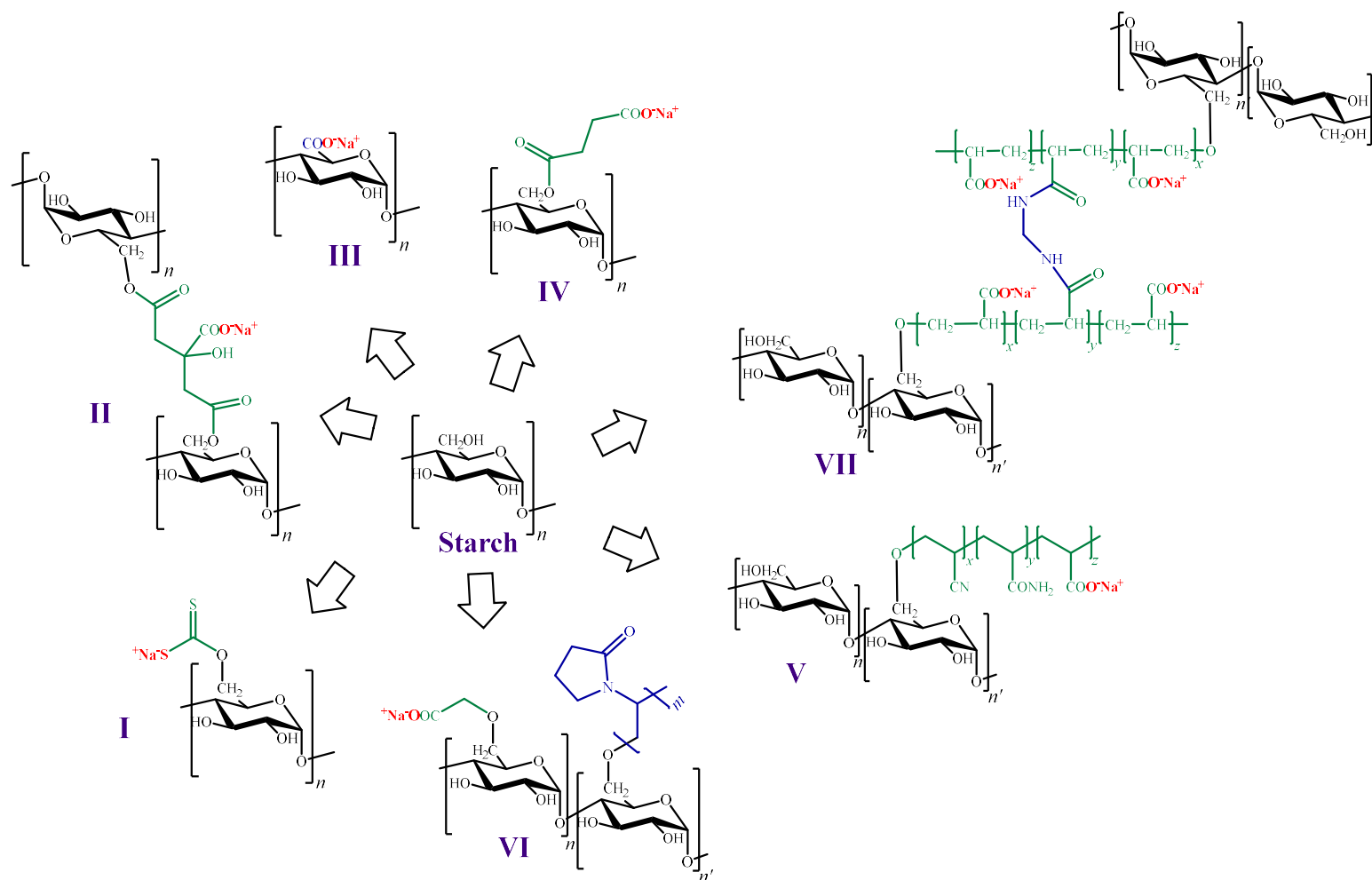


Figure 15. Chemical structures of cation exchangers derived from starch.

There are also reports of materials prepared using acrylic acid as the grafting monomer. For instance, Bahadoran et al. [82] reported a starch-g-poly(acrylic acid) hydrogel, achieving 736.0 mg g^{-1} of Cu (II) removal. Additionally, cellulose nanofibers were incorporated into the hydrogel, which enhanced its adsorption capacity, obtaining a value of 957.0 mg g^{-1} of Cu (II).

Ma et al., also prepared a composite material from starch, obtaining a starch-graft-poly(acrylic acid)/organo-modified zeolite, which was assayed for Cr (III) adsorption. The adsorbent's removal of the mentioned metal was 651.4 mg g^{-1} [203].

Moreover, Chen et al. [204] prepared a starch-based high-performance adsorptive hydrogel by grafting polyacrylic acid onto starch, and then crosslinking it with *N,N'*-methylene-bisacrylamide (Figure 15VII). This adsorbent was employed to remove the organic cationic dye MB from effluents in which its concentration was high, yielding a maximum adsorption capacity value of 2967.7 mg g^{-1} .

Additionally, Shoaib et al. prepared a composite material using starch, acrylic acid, and activated carbon from the red alga *Pterocladia capillacea* with *N,N'*-methylenebisacrylamide as a crosslinker and ammonium persulphate as an initiator. The adsorbent was assayed for MB dye removal, achieving 1428.6 mg g^{-1} as the maximum adsorption capacity value [205].

On the other hand, anion exchangers have been obtained by incorporating positive charges into the starch structure by introducing amino groups, as discussed for the other polysaccharides included in this review.

In this context, Zhang et al. [206] obtained a guanidine-containing starch-based resin via chemical modification of starch's structure with arginine (Figure 16). The material was assayed for the adsorption of dyes. In particular, acid fuchsin, acid orange G, and acid blue 80 were studied, and maximum adsorption capacity values of 21.6, 21.5 and 33.4 mg g^{-1} , respectively, were obtained.

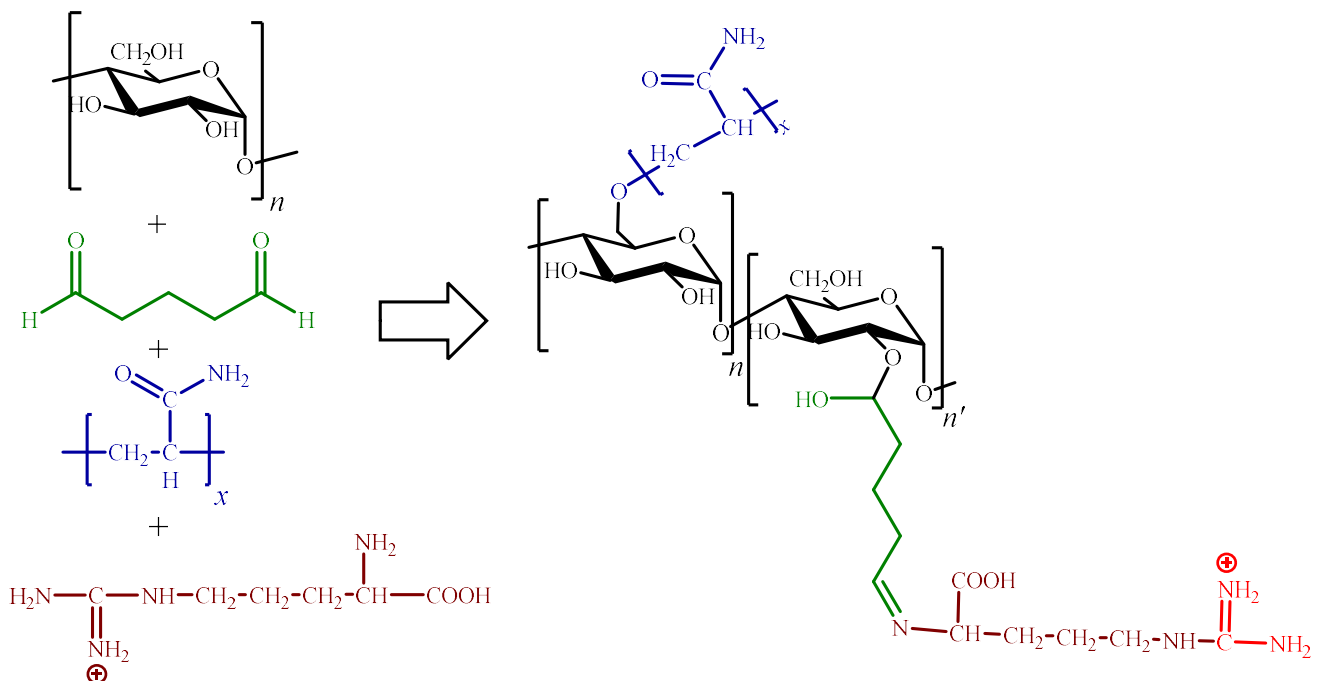


Figure 16. Starch chemical modifications described by Zhang et al. [206].

3. Discussion

Results presented along the review clearly show that polysaccharides are not suitable adsorbents in their native form due to low adsorption capacity and gel instability, among other traits. However, when polysaccharides are properly modified, the drawbacks mentioned can be overcome.

On the other hand, it is well known that polysaccharides' structure is variable and depends not only on the source from which each one is extracted, but also on environmental conditions. For instance, the content of G and M residues in alginates or starch composition (i.e., amylose and amylopectin proportions) are variable according to the season when sources are collected. Consequently, reproducibility of results could be affected considering such variations.

It is important to point out that reactivity to chemical modifications of polysaccharides can be enhanced by subjecting them to processes that increase the accessibility of reagents in their hydroxyl groups. For example, in the work of Gurgel et al. [100], the esterification degree of cellulose was significantly enhanced by carrying out a mercerization process, which reduced packing efficiency and increased the number of hydroxyl groups available for esterification.

It is noteworthy that the use of polysaccharides as support for highly adsorptive materials such as carbon nanotubes, GO, or other nanoparticles has a remarkable advantage: micro-sized water pollution is prevented.

Table 3 summarizes the materials addressed in this review that reached maximum adsorption capacity values that surpassed 200 mg g^{-1} ; these are grouped by the type of pollutant (i.e., heavy metals or dyes) and the raw material involved in each case, pH, adsorption kinetic and isotherm models are detailed. It is important to highlight that pH has a critical role in the adsorption process when either the adsorbents or pollutants are sensitive to it. For instance, when the adsorbent structure contains carboxylic groups, its adsorption capacity for cationic pollutants is highly increased at pH levels over 6, at which point this group, in their anionic form, can establish ionic interaction with cations. Conversely, in the case of adsorbents containing amino groups, the adsorption towards anionic pollutants is higher at pH levels below 5, at which point the protonation of the amino groups confers them a positive charge. In the case of pollutants, most dyes have acidic or basic properties, and therefore their structure and charge are pH-dependent, while heavy metals can form insoluble hydroxides at pH above 7 (e.g., Pb (II), Cu (II)).

Nevertheless, since adsorbents' efficiency could be related not only to the chemical structure of the adsorbent, but also to experimental conditions (such as temperature, adsorbent dose, contact time, initial concentration of the contaminant, among others), comparison between the results given for different authors should be carefully analysed.

Moreover, it is important to point out that, since heavy metals and dyes may have significantly different molecular weights, their adsorption capacity values are not worth comparing.

Table 3. Summary table including the materials described that in this review that have at least a maximum adsorption capacity value of 200 mg g⁻¹.

Pollutants	Raw Material	Product	Maximum Adsorption Capacity (mg g ⁻¹)	pH	Isotherm Model	Kinetic Model	Reference
<i>Heavy metals</i>							
As (III)	Cellulose	Activated carbon/carborundum/microcrystalline cellulose core shell nano-composite	422.9	6.0	Freundlich	Pseudo-second order	[79]
As (V)	Cellulose	Cellulose anion exchanger (graft polymerization of cellulose and glycidyl methacrylate)	200.3	6.0	Langmuir-Freundlich	Pseudo-second order	[107]
Cd (II)	Alginate and chitosan	Glutaraldehyde-crosslinked chitosan/alginate composite	220.5	5.8	Langmuir	Pseudo-first order	[175]
	Cellulose	Microcrystalline cellulose/bentonite grafted polyacrylic acid hydrogel	242.5	6.0	Freundlich	Pseudo-second order	[77]
Co (II)	Chitosan	Porous lignosulphonate/chitosan composite	386.0	6.0	Langmuir	Pseudo-second order	[166]
Cu (II)	Cellulose	Bamboo nanocellulose/montmorillonite nanosheets/polyethyleneimine gel adsorbent	254.6	5.0	Sips	Fractal-like pseudo-second order	[71]
	Cellulose	Activated carbon/carborundum/microcrystalline cellulose core shell nano-composite	423.6	6.0	Freundlich	Pseudo-second order	[79]
	Chitosan	Porous lignosulphonate/chitosan composite	283.0	6.0	Langmuir	Pseudo-second order	[166]
	Chitosan and cellulose	Zeolitic imidazolate framework-67 modified bacterial cellulose/chitosan composite aerogel	200.6	6.0	N/R	Pseudo-second order	[56]
	Starch	Starch-g-poly(acrylic acid) hydrogel	736.0				
	Starch and cellulose	Starch-g-poly(acrylic acid) hydrogel with cellulose nanofibers incorporated	957.0	5.0	Langmuir	N/R	[82]
Cr (III)	Starch	Starch-graft-poly(acrylic acid)/organo-modified zeolite	651.4	4.0	N/R	N/R	[203]

Table 3. Cont.

Pollutants	Raw Material	Product	Maximum Adsorption Capacity (mg g ⁻¹)	pH	Isotherm Model	Kinetic Model	Reference
Hg (II)	Cellulose	Citrate cellulose derivative	1600.0	6.5	Langmuir	Pseudo-second order	[102]
	Starch	Starch hydrogels prepared via graft polymerization of acrylonitrile, followed by nitrile groups hydrolysis	1250.0	4.0	Langmuir	Second order	[200]
Pb (II)	Alginate	Polyacrylamide/GO/sodium alginate composite	240.7	5.5	Langmuir	Pseudo-second order	[207]
		Thiol and amido-modified alginate/GO/composite	369.6	5.5	Langmuir	Pseudo-second order	[137]
		Sugarcane bagasse succinate/alginate composite	354.6	6.0	Langmuir	Pseudo-second order	[155]
	Cellulose	Cellulose crosslinked in presence of polyacrilamide	840.1	5.0	Langmuir	Pseudo-second order	[97]
		Titanium oxide-bacterial cellulose bioadsorbent	200.0	7.0	N/R	N/R	[74]
	Cellulose and alginate	Nanocrystalline cellulose/sodium alginate/K-carrageenan composite hydrogel	351.0	N/R	Langmuir	Pseudo-second order	[51]
		Glutaraldehyde crosslinked calcium alginate/cellulose bead	206.8	5.0	Freundlich	Pseudo-second order	[52]
	Chitosan and alginate	Glutaraldehyde-crosslinked chitosan/alginate composite	258.6	5.8	Sips	Pseudo-first order	[175]
	Chitosan	Porous lignosulphonate/chitosan composite	525.0	7.0	Langmuir	Pseudo-second order	[167]
	Starch	Starch hydrogels prepared via graft polymerization of acrylonitrile, followed by nitrile groups hydrolysis	264.4	5.0	Langmuir	Pseudo-first order	[201]

Table 3. Cont.

Pollutants	Raw Material	Product	Maximum Adsorption Capacity (mg g ⁻¹)	pH	Isotherm Model	Kinetic Model	Reference
<i>Dyes</i>							
Acid red	Cellulose	Amino-functionalized nanocrystalline cellulose	555.6	4.7	Langmuir	Pseudo-second order	[105]
AR13, AB92, AR112		Cationic cellulose hydrogels crosslinked with poly(ethylene glycol)	322.0–447.0	7.0	Langmuir	Pseudo-second order	[106]
Auramine O		Cellulose/montmorillonite mesoporous composite beads	1336.2	7.0	Redlich-Peterson	Pseudo-second order	[68]
Reactive yellow		Hyperbranched polyethyleneimine cellulose	970.87	5.0	Langmuir	Pseudo-second order	[104]
Crystal violet	Cellulose and alginate	Cellulose-based modified citrus peels/calcium alginate composite	882.0	6.5	Langmuir	Pseudo-second order	[50]
CR		Coffee ground cellulose/sodium alginate double-network hydrogel beads	411.5	N/R	Langmuir-Freundlich	Pseudo-second order	[54]
	Cellulose and chitosan	Cellulose/chitosan composite aerogel	381.7	7.0	Langmuir	Pseudo-second order	[57]
MB, rhodamine B, orange II, methyl orange	Alginate	Polyaniline-sodium alginate nanocomposite	416.7–555.5	7.0	Langmuir	Pseudo-second order	[132]
	Alginate	Alginate/rice husk composite	274.9	6.0	Freundlich	Fractal Brouers-Sotolongo	[148]
		Porous montmorillonite nanosheet/poly (acrylamide-co-acrylic acid)/sodium alginate hydrogel	530.7	6.8	Freundlich	Pseudo-second order	[151]
MB	Alginate and cellulose	Cellulose-based modified citrus peels/calcium alginate composite	923.1	6.5	Langmuir	Pseudo-second order	[50]
		Calcium alginate hydrogels reinforced with cellulose nanocrystals	676.7	7.0	Langmuir	Pseudo-first order	[53]
		Coffee ground cellulose/sodium alginate double-network hydrogel beads	400.5	N/R	Langmuir-Freundlich	Pseudo-second order	[54]

Table 3. Cont.

Pollutants	Raw Material	Product	Maximum Adsorption Capacity (mg g ⁻¹)	pH	Isotherm Model	Kinetic Model	Reference
	Cellulose	Cellulose crosslinked in presence of polyacrylamide	1611.4	5.0	Langmuir	Pseudo-second order	[97]
		Bamboo nanocellulose/montmorillonite nanosheets/polyethyleneimine gel adsorbent	361.9	10.0	Sips	Fractal-like pseudo-second order	[71]
		Graphene oxide incorporated into cellulose acetate beads	369.9	7.0	Langmuir	Pseudo-second order	[64]
	Chitosan and alginate	Chitosan/sodium alginate composite foam	1488.1	5.8	Langmuir	Pseudo-second order	[171]
	Starch	Starch, acrylic acid, and activated carbon from red alga <i>Pterocladia capillacea</i> with <i>N,N'</i> -methylenebisacrylamide/ammonium persulphate	1428.6	8.0	Langmuir	Pseudo-first order	[205]
		Starch-graft-polyacrylic acid, crosslinked with <i>N,N'</i> -methylene-bisacrylamide	2967.7	5.8	Langmuir	Pseudo-first order	[204]
		Starch-Ni/Fe-layered double hydroxide composite	387.6	3.0	Langmuir	Pseudo-second order	[190]
Methyl orange		Starch-modified ZnMgAl-layered doubled hydroxides	1555.0	7.0	Langmuir	Pseudo-second order	[191]
Rhodamine 6G		Carboxymethyl starch grafting with <i>N</i> -vinylpyrrolidone	363.9	5.0	N/R	N/R	[202]
Reactive blue 49	Chitosan	Chitosan crosslinked with citric acid esterified β -cyclodextrin	498.0	2.0	Langmuir	Pseudo-second order	[162]

4. Conclusions

From the analyses of the results presented along the manuscript, it can be concluded that higher maximum adsorption capacity values are related to the final products' chemical structure and not to the structure of the native polysaccharides.

Moreover, it is important to point out that most of the works summarized herein evaluate the adsorption capacity of the materials regarding certain pollutants in model aqueous systems, while complex matrixes such as wastewater samples have not been analysed so far. Therefore, as far as pollutant analysis is concerned, there is still a long way ahead for the industrial application of the adsorbents reported until now.

Furthermore, it is relevant to highlight that in all the analysed cases, materials were developed in laboratory scales and there is no economic analysis reported at all. Furthermore, most of the studies were only conducted in batches, and continuous column system analyses are still pending in many of the works included here. In this context, it is difficult to determine whether the materials could be scaled up or not to a pilot or industrial level, regarding both technical and economic feasibility. Nevertheless, it is important not to lose sight of the fact that, despite the need for column studies prior to scaling up, batch studies are the first step in the selection of novel materials that are worth submitting to deeper analyses as a means to the industrial scale.

All in all, researchers should continue to put in efforts towards scalability of the materials designed until now. In fact, a useful complementary tool for this feasibility analysis could be the use of computational modelling to predict the potential application of the designed materials in the adsorption process.

Author Contributions: G.D.B.: Investigation, Data curation, Visualization, Writing—original draft, Writing—review and editing. E.R.: Investigation, Data curation, Visualization, Writing—original draft, Writing—review and editing. M.I.E.: Conceptualization, Investigation, Data curation, Funding acquisition, Visualization, Writing—original draft, Writing—review and editing, Supervision. All authors have read and agreed to the published version of the manuscript.

Funding: This research was funded by the Agencia Nacional de Promoción Científica y Tecnológica (PICT2020-00221) and Instituto Tecnológico de Buenos Aires (ITBA).

Acknowledgments: Gema Díaz Bukvic has a fellowship from Consejo Nacional de Investigaciones Científicas y Técnicas (CONICET).

Conflicts of Interest: The authors declare no conflict of interest.

References

1. Khilchevskiy, V.K.; Oliinyk, Y.B.; Zatserkovnyi, V.I. Global problems of water resources scarcity. In Proceedings of the XIV International Scientific Conference “Monitoring of Geological Processes and Ecological Condition of the Environment”, Kyiv, Ukraine, 10 November 2020; pp. 1–5.
2. UNESCO World Water Assessment Programme. The United Nations World Water Development Report 2021: Valuing Water. Available online: <https://www.unesco.org/reports/wwdr/2021/en/download-report> (accessed on 30 June 2023).
3. Simonovic, S.P. World water dynamics: Global modeling of water resources. *J. Environ. Manag.* **2002**, *66*, 249–267. [[CrossRef](#)]
4. Kumar, V.; Kumar, S.; Américo-Pinheiro, J.H.P.; Vinthange, M.; Sher, F. Editorial: Emerging approaches for sustainable management for wastewater. *Front. Environ. Sci.* **2023**, *10*, 1122659. [[CrossRef](#)]
5. Skouteris, G.; Rodriguez-Garcia, G.; Reinecke, S.F.; Hampel, U. The use of pure oxygen for aeration in aerobic wastewater treatment: A review of its potential and limitations. *Bioresour. Technol.* **2020**, *312*, 123595. [[CrossRef](#)] [[PubMed](#)]
6. Cescon, A.; Jiang, J.-Q. Filtration process and alternative filter media material in water treatment. *Water* **2020**, *12*, 3377. [[CrossRef](#)]
7. Hube, S.; Eskafi, M.; Hrafnkelsdóttir, K.F.; Bjarnadóttir, B.; Bjarnadóttir, M.Á.; Axelsdóttir, S.; Wu, B. Direct membrane filtration for wastewater treatment and resource recovery: A review. *Sci. Total Environ.* **2020**, *710*, 136375. [[CrossRef](#)]
8. Ding, H.; Zhang, J.; He, H.; Zhu, Y.; Dionysiou, D.D.; Liu, Z.; Zhao, C. Do membrane filtration systems in drinking water treatment plants release nano/microplastics? *Sci. Total Environ.* **2021**, *755*, 142658. [[CrossRef](#)]

9. Chang, L.; Cao, Y.; Fan, G.; Li, C.; Peng, W. A review of the applications of ion floatation: Wastewater treatment, mineral beneficiation and hydrometallurgy. *RSC Adv.* **2019**, *9*, 20226–20239. [[CrossRef](#)]
10. Roy, A.; Thakur, B.; Debsarkar, A. Water Pollution and Treatment Technologies. In *Environmental Management: Issues and Concerns in Developing Countries*; Sikdar, P.K., Ed.; Springer International Publishing: Cham, Switzerland, 2021; pp. 79–106.
11. Kyzas, G.Z.; Matis, K.A. Flotation in Water and Wastewater Treatment. *Processes* **2018**, *6*, 116. [[CrossRef](#)]
12. Cui, H.; Huang, X.; Yu, Z.; Chen, P.; Cao, X. Application progress of enhanced coagulation in water treatment. *RSC Adv.* **2020**, *10*, 20231–20244. [[CrossRef](#)]
13. Zhao, C.; Zhou, J.; Yan, Y.; Yang, L.; Xing, G.; Li, H.; Wu, P.; Wang, M.; Zheng, H. Application of coagulation/flocculation in oily wastewater treatment: A review. *Sci. Total Environ.* **2021**, *765*, 142795. [[CrossRef](#)]
14. Sillanpää, M.; Ncibi, M.C.; Matilainen, A.; Vepsäläinen, M. Removal of natural organic matter in drinking water treatment by coagulation: A comprehensive review. *Chemosphere* **2018**, *190*, 54–71. [[CrossRef](#)] [[PubMed](#)]
15. Jumadi, J.; Kamari, A.; Hargreaves, J.S.J.; Yusof, N. A review of nano-based materials used as flocculants for water treatment. *Int. J. Environ. Sci. Technol.* **2020**, *17*, 3571–3594. [[CrossRef](#)]
16. Sookhak Lari, K.; Rayner, J.L.; Davis, G.B. Towards characterizing LNAPL remediation endpoints. *J. Environ. Manag.* **2018**, *224*, 97–105. [[CrossRef](#)]
17. Worthington, M.J.H.; Shearer, C.J.; Esdaile, L.J.; Campbell, J.A.; Gibson, C.T.; Legg, S.K.; Yin, Y.; Lundquist, N.A.; Gascooke, J.R.; Albuquerque, I.S.; et al. Sustainable polysulfides for oil spill remediation: Repurposing industrial waste for environmental benefit. *Adv. Sustain. Syst.* **2018**, *2*, 1800024. [[CrossRef](#)]
18. Rachmadi, A.T.; Kitajima, M.; Kato, T.; Kato, H.; Okabe, S.; Sano, D. Required Chlorination Doses to Fulfill the Credit Value for Disinfection of Enteric Viruses in Water: A Critical Review. *Environ. Sci. Technol.* **2020**, *54*, 2068–2077. [[CrossRef](#)]
19. Mazhar, M.A.; Khan, N.A.; Ahmed, S.; Khan, A.H.; Hussain, A.; Rahisuddin; Changani, F.; Yousefi, M.; Ahmadi, S.; Vambol, V. Chlorination disinfection by-products in municipal drinking water—A review. *J. Clean. Prod.* **2020**, *273*, 123159. [[CrossRef](#)]
20. Cimadoro, J.; Ribba, L.; Ledesma, S.; Goyanes, S. Electrospun mats: From white to transparent with a drop. *Macromol. Mater. Eng.* **2018**, *303*, 1800237. [[CrossRef](#)]
21. Pereira, P.P.; Fernandez, M.; Cimadoro, J.; González, P.S.; Morales, G.M.; Goyanes, S.; Agostini, E. Biohybrid membranes for effective bacterial vehiculation and simultaneous removal of hexavalent chromium (Cr VI) and phenol. *Appl. Microbiol. Biotechnol.* **2021**, *105*, 827–838. [[CrossRef](#)]
22. Cimadoro, J.; Goyanes, S. Reversible swelling as a strategy in the development of smart membranes from electrospun polyvinyl alcohol nanofiber mats. *J. Polym. Sci.* **2020**, *58*, 737–746. [[CrossRef](#)]
23. Wei, C.; Zhang, F.; Hu, Y.; Feng, C.; Wu, H. Ozonation in water treatment: The generation, basic properties of ozone and its practical application. *Rev. Chem. Eng.* **2017**, *33*, 49–89. [[CrossRef](#)]
24. Giuliani, L.; De Angelis, L.; Diaz Bukvic, G.; Zanini, M.; Minotti, F.; Errea, M.I.; Grondona, D. Trielectrode plasma reactor for water treatment. *J. Appl. Phys.* **2020**, *127*, 223303. [[CrossRef](#)]
25. Bermúdez, L.A.; Pascual, J.M.; Martínez, M.d.M.M.; Poyatos Capilla, J.M. Effectiveness of advanced oxidation processes in wastewater treatment: State of the art. *Water* **2021**, *13*, 2094. [[CrossRef](#)]
26. Abdullah, N.H.S.; Karsiti, M.N.; Ibrahim, R. A review of pH neutralization process control. In Proceedings of the 2012 4th International Conference on Intelligent and Advanced Systems (ICIAS2012), Kuala Lumpur, Malaysia, 12–14 June 2012; pp. 594–598.
27. Picón, D.; Torasso, N.; Baudrit, J.R.V.; Cervený, S.; Goyanes, S. Bio-inspired membranes for adsorption of arsenic via immobilized L-Cysteine in highly hydrophilic electrospun nanofibers. *Chem. Eng. Res. Des.* **2022**, *185*, 108–118. [[CrossRef](#)]
28. Saleh, T.A.; Mustaqeem, M.; Khaled, M. Water treatment technologies in removing heavy metal ions from wastewater: A review. *Environ. Nanotechnol. Monit. Manag.* **2022**, *17*, 100617. [[CrossRef](#)]
29. Fu, Z.-J.; Jiang, S.-K.; Chao, X.-Y.; Zhang, C.-X.; Shi, Q.; Wang, Z.-Y.; Liu, M.-L.; Sun, S.-P. Removing miscellaneous heavy metals by all-in-one ion exchange-nanofiltration membrane. *Water Res.* **2022**, *222*, 118888. [[CrossRef](#)]
30. Tran, T.V.; Nguyen, D.T.C.; Nguyen, T.T.T.; Nguyen, D.H.; Alhassan, M.; Jalil, A.A.; Nabgan, W.; Lee, T. A critical review on pineapple (*Ananas comosus*) wastes for water treatment, challenges and future prospects towards circular economy. *Sci. Total Environ.* **2023**, *856*, 158817. [[CrossRef](#)]
31. Huang, X.; Hadi, P.; Joshi, R.; Alhamzani, A.G.; Hsiao, B.S. A Comparative Study of Mechanism and Performance of Anionic and Cationic Dialdehyde Nanocelluloses for Dye Adsorption and Separation. *ACS Omega* **2023**, *8*, 8634–8649. [[CrossRef](#)]
32. Kennedy, K.K.; Maseka, K.J.; Mbulo, M. Selected adsorbents for removal of contaminants from wastewater: Towards engineering clay minerals. *Open J. Appl. Sci.* **2018**, *8*, 355–369. [[CrossRef](#)]
33. Bonilla-Petriciolet, A.; Mendoza-Castillo, D.I.; Reynel-Ávila, H.E. *Adsorption Processes for Water Treatment and Purification*; Springer: Cham, Switzerland, 2017; Volume 256.

34. Rossi, E.; Ramírez, J.A.Á.; Errea, M.I. Preparation of an environmentally friendly lead adsorbent. A contribution to the rational design of heavy metal adsorbents. *J. Environ. Chem. Eng.* **2020**, *8*, 104210. [[CrossRef](#)]
35. Atkins, P.W.; De Paula, J. *Atkins' Physical Chemistry*; Oxford University Press: Oxford, UK, 2014.
36. Dinh, V.-P.; Le, N.-C.; Tuyen, L.A.; Hung, N.Q.; Nguyen, V.-D.; Nguyen, N.-T. Insight into adsorption mechanism of lead(II) from aqueous solution by chitosan loaded MnO₂ nanoparticles. *Mater. Chem. Phys.* **2018**, *207*, 294–302. [[CrossRef](#)]
37. Errea, M.I.; Rossi, E.; Goyanes, S.N.; D'Accorso, N.B. Chitosan: From organic pollutants to high-value polymeric materials. In *Industrial Applications of Renewable Biomass Products*; Springer International Publishing: Cham, Switzerland, 2017; pp. 251–264.
38. Rossi, E.; Montoya Rojo, Ú.; Cerrutti, P.; Foresti, M.L.; Errea, M.I. Carboxymethylated bacterial cellulose: An environmentally friendly adsorbent for lead removal from water. *J. Environ. Chem. Eng.* **2018**, *6*, 6844–6852. [[CrossRef](#)]
39. Dambies, L.; Salinaro, R.; Alexandratos, S.D. Immobilized N-Methyl-d-glucamine as an Arsenate-Selective Resin. *Environ. Sci. Technol.* **2004**, *38*, 6139–6146. [[CrossRef](#)]
40. Crini, G.; Lichtfouse, E.; Wilson, L.D.; Morin-Crini, N. Conventional and non-conventional adsorbents for wastewater treatment. *Environ. Chem. Lett.* **2019**, *17*, 195–213. [[CrossRef](#)]
41. Pennells, J.; Godwin, I.D.; Amiralian, N.; Martin, D.J. Trends in the production of cellulose nanofibers from non-wood sources. *Cellulose* **2020**, *27*, 575–593. [[CrossRef](#)]
42. Heinze, T.; El Seoud, O.A.; Koschella, A. Production and Characteristics of Cellulose from Different Sources. In *Cellulose Derivatives: Synthesis, Structure, and Properties*; Heinze, T., El Seoud, O.A., Koschella, A., Eds.; Springer International Publishing: Cham, Switzerland, 2018; pp. 1–38.
43. Rossi, E.; Salvay, A.G.; Errea, M.I.; Foresti, M.L. Dried water-redispersible bacterial nanocellulose with sorbitol as capping agent. *Food Hydrocoll.* **2023**, *143*, 108916. [[CrossRef](#)]
44. Bovi, J.; Butto, M.; Arroyo, S.; Bernal, C.; Foresti, M.L. Bacterial Cellulose nanofibrils from a By-Product of the Growing Kombucha Business: Obtention and Use in the Development of Poly (Lactic Acid) Composites. *Lat. Am. Appl. Res.* **2023**, *in press*.
45. Dima, S.-O.; Panaitescu, D.-M.; Orban, C.; Ghiurea, M.; Doncea, S.-M.; Fierascu, R.C.; Nistor, C.L.; Alexandrescu, E.; Nicolae, C.-A.; Trică, B.; et al. Bacterial Nanocellulose from Side-Streams of Kombucha Beverages Production: Preparation and Physical-Chemical Properties. *Polymers* **2017**, *9*, 374. [[CrossRef](#)]
46. Gupta, V.K.; Carrott, P.J.M.; Singh, R.; Chaudhary, M.; Kushwaha, S. Cellulose: A review as natural, modified and activated carbon adsorbent. *Bioresour. Technol.* **2016**, *216*, 1066–1076. [[CrossRef](#)]
47. Hokkanen, S.; Bhatnagar, A.; Sillanpää, M. A review on modification methods to cellulose-based adsorbents to improve adsorption capacity. *Water Res.* **2016**, *91*, 156–173. [[CrossRef](#)]
48. Marimuthu, T.; Chee, C.Y.; Sulaiman, N.M.N. A review on the use of cellulose nanomaterials for wastewater remediation of heavy metal ions. *Int. J. Environ. Sci. Technol.* **2023**, *20*, 3421–3436. [[CrossRef](#)]
49. He, Z.; Song, H.; Cui, Y.; Zhu, W.; Du, K.; Yao, S. Porous Spherical Cellulose Carrier Modified with Polyethyleneimine and Its Adsorption for Cr(III) and Fe(III) from Aqueous Solutions. *Chin. J. Chem. Eng.* **2014**, *22*, 984–990. [[CrossRef](#)]
50. Aichour, A.; Zaghouane-Boudiaf, H. Single and competitive adsorption studies of two cationic dyes from aqueous mediums onto cellulose-based modified citrus peels/calcium alginate composite. *Int. J. Biol. Macromol.* **2020**, *154*, 1227–1236. [[CrossRef](#)] [[PubMed](#)]
51. Shen, J.; Xu, X.; Ouyang, X.; Jin, M. Adsorption of Pb(II) from Aqueous Solutions Using Nanocrystalline Cellulose/Sodium Alginate/K-Carrageenan Composite Hydrogel Beads. *J. Polym. Environ.* **2022**, *30*, 1995–2006. [[CrossRef](#)]
52. Irvani Mohammadabadi, S.; Javanbakht, V. Fabrication of dual cross-linked spherical treated waste biomass/alginate adsorbent and its potential for efficient removal of lead ions from aqueous solutions. *Ind. Crop. Prod.* **2021**, *168*, 113575. [[CrossRef](#)]
53. Soleimani, S.; Heydari, A.; Fattahi, M.; Motamedisade, A. Calcium alginate hydrogels reinforced with cellulose nanocrystals for methylene blue adsorption: Synthesis, characterization, and modelling. *Ind. Crop. Prod.* **2023**, *192*, 115999. [[CrossRef](#)]
54. Kasbaji, M.; Mennani, M.; Grimi, N.; Oubenali, M.; Mbarki, M.; El Zakhem, H.; Moubarik, A. Adsorption of cationic and anionic dyes onto coffee grounds cellulose/sodium alginate double-network hydrogel beads: Isotherm analysis and recyclability performance. *Int. J. Biol. Macromol.* **2023**, *239*, 124288. [[CrossRef](#)]
55. Wu, J.; Dong, Z.; Li, X.; Li, P.; Wei, J.; Hu, M.; Geng, L.; Peng, X. Constructing acid-resistant chitosan/cellulose nanofibrils composite membrane for the adsorption of methylene blue. *J. Environ. Chem. Eng.* **2022**, *10*, 107754. [[CrossRef](#)]
56. Li, D.; Tian, X.; Wang, Z.; Guan, Z.; Li, X.; Qiao, H.; Ke, H.; Luo, L.; Wei, Q. Multifunctional adsorbent based on metal-organic framework modified bacterial cellulose/chitosan composite aerogel for high efficient removal of heavy metal ion and organic pollutant. *Chem. Eng. J.* **2020**, *383*, 123127. [[CrossRef](#)]
57. Wang, Y.; Wang, H.; Peng, H.; Wang, Z.; Wu, J.; Liu, Z. Dye Adsorption from Aqueous Solution by Cellulose/Chitosan Composite: Equilibrium, Kinetics, and Thermodynamics. *Fibers Polym.* **2018**, *19*, 340–349. [[CrossRef](#)]
58. Liu, K.; Chen, L.; Huang, L.; Lai, Y. Evaluation of ethylenediamine-modified nanofibrillated cellulose/chitosan composites on adsorption of cationic and anionic dyes from aqueous solution. *Carbohydr. Polym.* **2016**, *151*, 1115–1119. [[CrossRef](#)]

59. Liu, C.; Yu, J.; You, J.; Wang, Z.; Zhang, M.; Shi, L.; Zhuang, X. Cellulose/Chitosan Composite Sponge for Efficient Protein Adsorption. *Ind. Eng. Chem. Res.* **2021**, *60*, 9159–9166. [[CrossRef](#)]
60. Marrane, S.E.; Dänoun, K.; Allouss, D.; Sair, S.; Channab, B.-E.; Rhihil, A.; Zahouily, M. A Novel Approach to Prepare Cellulose-g-Hydroxyapatite Originated from Natural Sources as an Efficient Adsorbent for Heavy Metals: Batch Adsorption Optimization via Response Surface Methodology. *ACS Omega* **2022**, *7*, 28076–28092. [[CrossRef](#)] [[PubMed](#)]
61. Saber-Samandari, S.; Saber-Samandari, S.; Gazi, M. Cellulose-graft-polyacrylamide/hydroxyapatite composite hydrogel with possible application in removal of Cu (II) ions. *React. Funct. Polym.* **2013**, *73*, 1523–1530. [[CrossRef](#)]
62. Jin, Y.; Ni, Y.; Pudukudy, M.; Zhang, H.; Wang, H.; Jia, Q.; Shan, S. Synthesis of nanocrystalline cellulose/hydroxyapatite nanocomposites for the efficient removal of chlortetracycline hydrochloride in aqueous medium. *Mater. Chem. Phys.* **2022**, *275*, 125135. [[CrossRef](#)]
63. Mututvari, T.M.; Tran, C.D. Synergistic adsorption of heavy metal ions and organic pollutants by supramolecular polysaccharide composite materials from cellulose, chitosan and crown ether. *J. Hazard. Mater.* **2014**, *264*, 449–459. [[CrossRef](#)]
64. Eltaweil, A.S.; Abd El-Monaem, E.M.; El-Subruiti, G.M.; Ali, B.M.; Abd El-Latif, M.M.; Omer, A.M. Graphene oxide incorporated cellulose acetate beads for efficient removal of methylene blue dye; isotherms, kinetic, mechanism and co-existing ions studies. *J. Porous Mater.* **2023**, *30*, 607–618. [[CrossRef](#)]
65. Ogunleye, D.T.; Akpotu, S.O.; Moodley, B. Crystalline Nanocellulose Anchored on Reduced Graphene Oxide for the Removal of Pharmaceuticals from Aqueous Systems: Adsorbent Characterization and Adsorption Performance. *ChemistrySelect* **2023**, *8*, e202202533. [[CrossRef](#)]
66. Abou-Zeid, R.E.; Kamal, K.H.; Abd El-Aziz, M.E.; Morsi, S.M.; Kamel, S. Grafted TEMPO-oxidized cellulose nanofiber embedded with modified magnetite for effective adsorption of lead ions. *Int. J. Biol. Macromol.* **2021**, *167*, 1091–1101. [[CrossRef](#)]
67. Anugrahwati, M.; Sari, A.W.; Munawwaroh, L.A.; Musawwa, M.M. Synthesis of microcrystalline cellulose (MCC)-Fe₃O₄ for malachite green adsorption; kinetics, isotherms, thermodynamics, and regeneration studies. *J. Eng. Sci. Technol.* **2022**, *17*, 91–101.
68. Pan, Y.; Xie, H.; Liu, H.; Cai, P.; Xiao, H. Novel cellulose/montmorillonite mesoporous composite beads for dye removal in single and binary systems. *Bioresour. Technol.* **2019**, *286*, 121366. [[CrossRef](#)]
69. Rong, N.; Chen, C.; Ouyang, K.; Zhang, K.; Wang, X.; Xu, Z. Adsorption characteristics of directional cellulose nanofiber/chitosan/montmorillonite aerogel as adsorbent for wastewater treatment. *Sep. Purif. Technol.* **2021**, *274*, 119120. [[CrossRef](#)]
70. Luo, J.; Ma, X.; Zhou, X.; Xu, Y. Construction of physically crosslinked cellulose nanofibrils/alkali lignin/montmorillonite/polyvinyl alcohol network hydrogel and its application in methylene blue removal. *Cellulose* **2021**, *28*, 5531–5543. [[CrossRef](#)]
71. Zhang, X.; Li, F.; Zhao, X.; Cao, J.; Liu, S.; Zhang, Y.; Yuan, Z.; Huang, X.; De Hoop, C.F.; Peng, X.; et al. Bamboo Nanocellulose/Montmorillonite Nanosheets/Polyethyleneimine Gel Adsorbent for Methylene Blue and Cu(II) Removal from Aqueous Solutions. *Gels* **2023**, *9*, 40. [[CrossRef](#)] [[PubMed](#)]
72. Kumar, A.S.K.; Kalidhasan, S.; Rajesh, V.; Rajesh, N. Application of Cellulose-Clay Composite Biosorbent toward the Effective Adsorption and Removal of Chromium from Industrial Wastewater. *Ind. Eng. Chem. Res.* **2012**, *51*, 58–69. [[CrossRef](#)]
73. Cai, J.; Lei, M.; Zhang, Q.; He, J.-R.; Chen, T.; Liu, S.; Fu, S.-H.; Li, T.-T.; Liu, G.; Fei, P. Electrospun composite nanofiber mats of Cellulose@Organically modified montmorillonite for heavy metal ion removal: Design, characterization, evaluation of adsorption performance. *Compos. Part A Appl. Sci. Manuf.* **2017**, *92*, 10–16. [[CrossRef](#)]
74. Shoukat, A.; Wahid, F.; Khan, T.; Siddique, M.; Nasreen, S.; Yang, G.; Ullah, M.W.; Khan, R. Titanium oxide-bacterial cellulose bioadsorbent for the removal of lead ions from aqueous solution. *Int. J. Biol. Macromol.* **2019**, *129*, 965–971. [[CrossRef](#)]
75. Jing, L.; Yang, S.; Li, X.; Jiang, Y.; Lou, J.; Liu, Z.; Ding, Q.; Han, W. Effective adsorption and sensitive detection of Cr⁶⁺ by degradable collagen-based porous fluorescent aerogel. *Ind. Crop. Prod.* **2022**, *182*, 114882. [[CrossRef](#)]
76. Shamsudin, M.S.; Azha, S.F.; Shahadat, M.; Ismail, S. Cellulose/bentonite-zeolite composite adsorbent material coating for treatment of N-based antiseptic cationic dye from water. *J. Water Process Eng.* **2019**, *29*, 100764. [[CrossRef](#)]
77. Ding, W.; Liang, H.; Zhang, H.; Sun, H.; Geng, Z.; Xu, C. A cellulose/bentonite grafted polyacrylic acid hydrogel for highly-efficient removal of Cd(II). *J. Water Process Eng.* **2023**, *51*, 103414. [[CrossRef](#)]
78. Xu, D.; Huang, Y.; Ma, Q.; Qiao, J.; Guo, X.; Wu, Y. A 3D porous structured cellulose nanofibrils-based hydrogel with carbon dots-enhanced synergetic effects of adsorption and photocatalysis for effective Cr(VI) removal. *Chem. Eng. J.* **2023**, *456*, 141104. [[CrossRef](#)]
79. Mubarak, M.F.; Zayed, A.M.; Ahmed, H.A. Activated Carbon/Carborundum@Microcrystalline Cellulose core shell nanocomposite: Synthesis, characterization and application for heavy metals adsorption from aqueous solutions. *Ind. Crop. Prod.* **2022**, *182*, 114896. [[CrossRef](#)]
80. Zhao, B.; Jiang, H.; Lin, Z.; Xu, S.; Xie, J.; Zhang, A. Preparation of acrylamide/acrylic acid cellulose hydrogels for the adsorption of heavy metal ions. *Carbohydr. Polym.* **2019**, *224*, 115022. [[CrossRef](#)]
81. Guleria, A.; Kumari, G.; Lima, E.C. Cellulose-g-poly-(acrylamide-co-acrylic acid) polymeric bioadsorbent for the removal of toxic inorganic pollutants from wastewaters. *Carbohydr. Polym.* **2020**, *228*, 115396. [[CrossRef](#)]

82. Bahadoran Baghbadorani, N.; Behzad, T.; Etesami, N.; Heidarian, P. Removal of Cu²⁺ ions by cellulose nanofibers-assisted starch-g-poly(acrylic acid) superadsorbent hydrogels. *Compos. Part B Eng.* **2019**, *176*, 107084. [[CrossRef](#)]
83. Malatji, N.; Makhado, E.; Ramohlola, K.E.; Modibane, K.D.; Maponya, T.C.; Monama, G.R.; Hato, M.J. Synthesis and characterization of magnetic clay-based carboxymethyl cellulose-acrylic acid hydrogel nanocomposite for methylene blue dye removal from aqueous solution. *Environ. Sci. Pollut. Res.* **2020**, *27*, 44089–44105. [[CrossRef](#)]
84. Godiya, C.B.; Cheng, X.; Li, D.; Chen, Z.; Lu, X. Carboxymethyl cellulose/polyacrylamide composite hydrogel for cascaded treatment/reuse of heavy metal ions in wastewater. *J. Hazard. Mater.* **2019**, *364*, 28–38. [[CrossRef](#)]
85. El Fawal, G.; Khalifa, R.; Rahman, S.A.; Eldin, M.M. Poly (Methacrylic acid) grafted regenerated cellulose ions exchangers membranes for Cu (II) ion adsorption: Kinetic, isotherm, and thermodynamic studies. *Desalination Water Treat.* **2020**, *178*, 182–192. [[CrossRef](#)]
86. Abouzayed, F.I.; El-Nasser, N.T.A.; Abouel-Enein, S.A. Synthesis, characterization of functionalized grafted cellulose and its environmental application in uptake of copper (II), manganese (II) and iron (III) ions. *J. Mol. Struct.* **2022**, *1270*, 133907. [[CrossRef](#)]
87. Rahman, M.L.; Fui, C.J.; Ting, T.X.; Sarjadi, M.S.; Arshad, S.E.; Musta, B. Polymer Ligands Derived from Jute Fiber for Heavy Metal Removal from Electroplating Wastewater. *Polymers* **2020**, *12*, 2521. [[CrossRef](#)]
88. Kumar, R.; Sharma, R.K.; Singh, A.P. Synthesis and characterization of cellulose based graft copolymers with binary vinyl monomers for efficient removal of cationic dyes and Pb(II) ions. *J. Polym. Res.* **2019**, *26*, 135. [[CrossRef](#)]
89. Kedzior, S.A.; Zoppe, J.O.; Berry, R.M.; Cranston, E.D. Recent advances and an industrial perspective of cellulose nanocrystal functionalization through polymer grafting. *Curr. Opin. Solid State Mater. Sci.* **2019**, *23*, 74–91. [[CrossRef](#)]
90. Wojnárovits, L.; Földváry, C.M.; Takács, E. Radiation-induced grafting of cellulose for adsorption of hazardous water pollutants: A review. *Radiat. Phys. Chem.* **2010**, *79*, 848–862. [[CrossRef](#)]
91. Feng, C.; Ren, P.; Huo, M.; Dai, Z.; Liang, D.; Jin, Y.; Ren, F. Facile synthesis of trimethylammonium grafted cellulose foams with high capacity for selective adsorption of anionic dyes from water. *Carbohydr. Polym.* **2020**, *241*, 116369. [[CrossRef](#)] [[PubMed](#)]
92. Fakhre, N.A.; Ibrahim, B.M. The use of new chemically modified cellulose for heavy metal ion adsorption. *J. Hazard. Mater.* **2018**, *343*, 324–331. [[CrossRef](#)]
93. Serbanescu, O.S.; Pandele, A.M.; Oprea, M.; Semenescu, A.; Thakur, V.K.; Voicu, S.I. Crown Ether-Immobilized Cellulose Acetate Membranes for the Retention of Gd (III). *Polymers* **2021**, *13*, 3978. [[CrossRef](#)]
94. Gupta, A.D.; Pandey, S.; Jaiswal, V.K.; Bhadauria, V.; Singh, H. Simultaneous oxidation and esterification of cellulose for use in treatment of water containing Cu(II) ions. *Carbohydr. Polym.* **2019**, *222*, 114964. [[CrossRef](#)]
95. Montoya Rojo, Ú.; Rossi, E.; Cerrutti, P.; Errea, M.I.; Foresti, M.L. Preparation of water insoluble carboxymethylated bacterial cellulose with maximum lead retention capacity. *J. Polym. Res.* **2021**, *28*, 212. [[CrossRef](#)]
96. Wei, W.; Kim, S.; Song, M.-H.; Bediako, J.K.; Yun, Y.-S. Carboxymethyl cellulose fiber as a fast binding and biodegradable adsorbent of heavy metals. *J. Taiwan Inst. Chem. Eng.* **2015**, *57*, 104–110. [[CrossRef](#)]
97. Chen, Y.; Long, Y.; Li, Q.; Chen, X.; Xu, X. Synthesis of high-performance sodium carboxymethyl cellulose-based adsorbent for effective removal of methylene blue and Pb (II). *Int. J. Biol. Macromol.* **2019**, *126*, 107–117. [[CrossRef](#)]
98. Baiya, C.; Nannuan, L.; Tassanapukdee, Y.; Chailapakul, O.; Songsrirote, K. The Synthesis of Carboxymethyl Cellulose-Based Hydrogel from Sugarcane Bagasse Using Microwave-Assisted Irradiation for Selective Adsorption of Copper(II) Ions. *Environ. Prog. Sustain. Energy* **2019**, *38*, S157–S165. [[CrossRef](#)]
99. Lin, X.; Jin, J.; Guo, X.; Jia, X. All-carboxymethyl cellulose sponges for removal of heavy metal ions. *Cellulose* **2021**, *28*, 3113–3122. [[CrossRef](#)]
100. Gurgel, L.V.A.; de Freitas, R.P.; Gil, L.F. Adsorption of Cu(II), Cd(II), and Pb(II) from aqueous single metal solutions by sugarcane bagasse and mercerized sugarcane bagasse chemically modified with succinic anhydride. *Carbohydr. Polym.* **2008**, *74*, 922–929. [[CrossRef](#)]
101. Olivito, F.; Algieri, V.; Jiritano, A.; Tallarida, M.A.; Tursi, A.; Costanzo, P.; Maiuolo, L.; De Nino, A. Cellulose citrate: A convenient and reusable bio-adsorbent for effective removal of methylene blue dye from artificially contaminated water. *RSC Adv.* **2021**, *11*, 34309–34318. [[CrossRef](#)] [[PubMed](#)]
102. Tursi, A.; Gallizzi, V.; Olivito, F.; Algieri, V.; De Nino, A.; Maiuolo, L.; Beneduci, A. Selective and efficient mercury(II) removal from water by adsorption with a cellulose citrate biopolymer. *JHM Lett.* **2022**, *3*, 100060. [[CrossRef](#)]
103. Shahid, M.K.; Dayarathne, H.N.P.; Mainali, B.; Lim, J.W.; Choi, Y. Ion Exchange Process for Removal of Microconstituents from Water and Wastewater. In *Microconstituents in the Environment*; John Wiley & Sons, Inc.: Hoboken, NJ, USA, 2023; pp. 303–320.
104. Chen, X.; Liu, L.; Luo, Z.; Shen, J.; Ni, Q.; Yao, J. Facile preparation of a cellulose-based bioadsorbent modified by hPEI in heterogeneous system for high-efficiency removal of multiple types of dyes. *React. Funct. Polym.* **2018**, *125*, 77–83. [[CrossRef](#)]
105. Jin, L.; Li, W.; Xu, Q.; Sun, Q. Amino-functionalized nanocrystalline cellulose as an adsorbent for anionic dyes. *Cellulose* **2015**, *22*, 2443–2456. [[CrossRef](#)]

106. Kono, H.; Ogasawara, K.; Kusumoto, R.; Oshima, K.; Hashimoto, H.; Shimizu, Y. Cationic cellulose hydrogels cross-linked by poly(ethylene glycol): Preparation, molecular dynamics, and adsorption of anionic dyes. *Carbohydr. Polym.* **2016**, *152*, 170–180. [[CrossRef](#)]
107. Anirudhan, T.S.; Jalajamony, S. Cellulose-based anion exchanger with tertiary amine functionality for the extraction of arsenic(V) from aqueous media. *J. Environ. Manag.* **2010**, *91*, 2201–2207. [[CrossRef](#)]
108. Pereira, A.R.; Soares, L.C.; Teodoro, F.S.; Elias, M.M.C.; Ferreira, G.M.D.; Savedra, R.M.L.; Siqueira, M.F.; Martineau-Corcós, C.; da Silva, L.H.M.; Prim, D.; et al. Aminated cellulose as a versatile adsorbent for batch removal of As(V) and Cu(II) from mono- and multicomponent aqueous solutions. *J. Colloid Interface Sci.* **2020**, *576*, 158–175. [[CrossRef](#)]
109. Dong, Z.; Zhao, L. Surface modification of cellulose microsphere with imidazolium-based ionic liquid as adsorbent: Effect of anion variation on adsorption ability towards Au(III). *Cellulose* **2018**, *25*, 2205–2216. [[CrossRef](#)]
110. Guo, W.; Yang, F.; Zhao, Z.; Liao, Q.; Cai, C.; Zhang, Y.; Bai, R. Cellulose-based ionic liquids as an adsorbent for high selective recovery of gold. *Miner. Eng.* **2018**, *125*, 271–278. [[CrossRef](#)]
111. Zhang, W.; Yang, G.; Deng, F.; Liang, J.; Huang, Q.; Dou, J.; Liu, M.; Cao, Q.-Y.; Zhang, X.; Wei, Y. Direct grafting of cellulose nanocrystals with poly(ionic liquids) via Gamma-ray irradiation and their utilization for adsorptive removal of CR. *Int. J. Biol. Macromol.* **2022**, *194*, 1029–1037. [[CrossRef](#)] [[PubMed](#)]
112. Chen, L.; Dai, Y.; Lu, Q.; Fang, C.; Wang, Z.; Li, Y.; Cai, L.; Liu, B.; Zhang, Y.-F.; Li, Y.; et al. Novel High-efficiency adsorbent consisting of magnetic Cellulose-based ionic liquid for removal of anionic dyes. *J. Mol. Liq.* **2022**, *353*, 118723.
113. Li, B.; Zhang, Q.; Pan, Y.; Li, Y.; Huang, Z.; Li, M.; Xiao, H. Functionalized porous magnetic cellulose/Fe₃O₄ beads prepared from ionic liquid for removal of dyes from aqueous solution. *Int. J. Biol. Macromol.* **2020**, *163*, 309–316. [[CrossRef](#)] [[PubMed](#)]
114. Wan, Y.; Liu, Z.-Y.; Song, P.; Zhang, X.-Q.; Song, J.-C.; Fu, Y.-J.; Yao, X.-H.; Wang, J.; Chen, T.; Zhang, D.-Y.; et al. Ionic liquid groups modified 3D porous cellulose microspheres for selective adsorption of AO7 dye. *J. Clean. Prod.* **2019**, *240*, 118201. [[CrossRef](#)]
115. Zhang, S.-F.; Yang, M.-X.; Qian, L.-W.; Hou, C.; Tang, R.-H.; Yang, J.-F.; Wang, X.-C. Design and preparation of a cellulose-based adsorbent modified by imidazolium ionic liquid functional groups and their studies on anionic dye adsorption. *Cellulose* **2018**, *25*, 3557–3569. [[CrossRef](#)]
116. Zhou, H.; Zhu, H.; Xue, F.; He, H.; Wang, S. Cellulose-based amphoteric adsorbent for the complete removal of low-level heavy metal ions via a specialization and cooperation mechanism. *Chem. Eng. J.* **2020**, *385*, 123879. [[CrossRef](#)]
117. Zhong, Q.-Q.; Yue, Q.-Y.; Li, Q.; Gao, B.-Y.; Xu, X. Removal of Cu(II) and Cr(VI) from wastewater by an amphoteric sorbent based on cellulose-rich biomass. *Carbohydr. Polym.* **2014**, *111*, 788–796. [[CrossRef](#)]
118. Kono, H. Preparation and Characterization of Amphoteric Cellulose Hydrogels as Adsorbents for the Anionic Dyes in Aqueous Solutions. *Gels* **2015**, *1*, 94–116. [[CrossRef](#)]
119. Zhu, T.; Li, Y.; Yang, H.; Liu, J.; Tao, Y.; Gan, W.; Wang, S.; Nong, G. Preparation of an amphoteric adsorbent from cellulose for wastewater treatment. *React. Funct. Polym.* **2021**, *169*, 105086. [[CrossRef](#)]
120. Draget, K.I. 29–Alginates. In *Handbook of Hydrocolloids*, 2nd ed.; Phillips, G.O., Williams, P.A., Eds.; Woodhead Publishing: Sawston, UK, 2009; pp. 807–828.
121. Hasnain, M.S.; Jameel, E.; Mohanta, B.; Dhara, A.K.; Alkahtani, S.; Nayak, A.K. Chapter 1–Alginates: Sources, structure, and properties. In *Alginates in Drug Delivery*; Nayak, A.K., Hasnain, M.S., Eds.; Academic Press: Cambridge, MA, USA, 2020; pp. 1–17.
122. Saji, S.; Hebden, A.; Goswami, P.; Du, C. A Brief Review on the Development of Alginate Extraction Process and Its Sustainability. *Sustainability* **2022**, *14*, 5181. [[CrossRef](#)]
123. Andriamanantoanina, H.; Rinaudo, M. Characterization of the alginates from five madagascan brown algae. *Carbohydr. Polym.* **2010**, *82*, 555–560. [[CrossRef](#)]
124. Cao, L.; Lu, W.; Mata, A.; Nishinari, K.; Fang, Y. Egg-box model-based gelation of alginate and pectin: A review. *Carbohydr. Polym.* **2020**, *242*, 116389. [[CrossRef](#)] [[PubMed](#)]
125. Hecht, H.; Srebnik, S. Structural Characterization of Sodium Alginate and Calcium Alginate. *Biomacromolecules* **2016**, *17*, 2160–2167. [[CrossRef](#)]
126. He, J.; Chen, J.P. A comprehensive review on biosorption of heavy metals by algal biomass: Materials, performances, chemistry, and modeling simulation tools. *Bioresour. Technol.* **2014**, *160*, 67–78. [[CrossRef](#)]
127. Papageorgiou, S.K.; Katsaros, F.K.; Kouvelos, E.P.; Nolan, J.W.; Le Deit, H.; Kanellopoulos, N.K. Heavy metal sorption by calcium alginate beads from *Laminaria digitata*. *J. Hazard. Mater.* **2006**, *137*, 1765–1772. [[CrossRef](#)]
128. Park, H.G.; Chae, M.Y. Novel type of alginate gel-based adsorbents for heavy metal removal. *J. Chem. Technol. Biotechnol.* **2004**, *79*, 1080–1083. [[CrossRef](#)]
129. Vijaya, Y.; Popuri, S.R.; Boddu, V.M.; Krishnaiah, A. Modified chitosan and calcium alginate biopolymer sorbents for removal of nickel (II) through adsorption. *Carbohydr. Polym.* **2008**, *72*, 261–271. [[CrossRef](#)]
130. Jeon, C.; Park, J.Y.; Yoo, Y.J. Novel immobilization of alginate acid for heavy metal removal. *Biochem. Eng. J.* **2002**, *11*, 159–166. [[CrossRef](#)]

131. Wang, W.; Kang, Y.; Wang, A. One-step fabrication in aqueous solution of a granular alginate-based hydrogel for fast and efficient removal of heavy metal ions. *J. Polym. Res.* **2013**, *20*, 101. [[CrossRef](#)]
132. Majhi, D.; Patra, B.N. Polyaniline and sodium alginate nanocomposite: A pH-responsive adsorbent for the removal of organic dyes from water. *RSC Adv.* **2020**, *10*, 43904–43914. [[CrossRef](#)]
133. Pashaei-Fakhri, S.; Peighambaroust, S.J.; Foroutan, R.; Arsalani, N.; Ramavandi, B. Crystal violet dye sorption over acrylamide/graphene oxide bonded sodium alginate nanocomposite hydrogel. *Chemosphere* **2021**, *270*, 129419. [[CrossRef](#)] [[PubMed](#)]
134. Peighambaroust, S.J.; Aghamohammadi-Bavil, O.; Foroutan, R.; Arsalani, N. Removal of malachite green using carboxymethyl cellulose-g-polyacrylamide/montmorillonite nanocomposite hydrogel. *Int. J. Biol. Macromol.* **2020**, *159*, 1122–1131. [[CrossRef](#)]
135. Zhang, W.; Ou, J.; Wang, B.; Wang, H.; He, Q.; Song, J.; Zhang, H.; Tang, M.; Zhou, L.; Gao, Y.; et al. Efficient heavy metal removal from water by alginate-based porous nanocomposite hydrogels: The enhanced removal mechanism and influencing factor insight. *J. Hazard. Mater.* **2021**, *418*, 126358. [[CrossRef](#)] [[PubMed](#)]
136. Majdoub, M.; Amedlous, A.; Anfar, Z.; Jada, A.; El Alem, N. Engineering of amine-based binding chemistry on functionalized graphene oxide/alginate hybrids for simultaneous and efficient removal of trace heavy metals: Towards drinking water. *J. Colloid Interface Sci.* **2021**, *589*, 511–524. [[CrossRef](#)] [[PubMed](#)]
137. Zhang, H.; Han, X.; Liu, J.; Wang, M.; Zhao, T.; Kang, L.; Zhong, S.; Cui, X. Fabrication of modified alginate-based biocomposite hydrogel microspheres for efficient removal of heavy metal ions from water. *Colloids Surf. Physicochem. Eng. Asp.* **2022**, *651*, 129736. [[CrossRef](#)]
138. Ihsanullah, I.; Sajid, M.; Khan, S.; Bilal, M. Aerogel-based adsorbents as emerging materials for the removal of heavy metals from water: Progress, challenges, and prospects. *Sep. Purif. Technol.* **2022**, *291*, 120923. [[CrossRef](#)]
139. Jiao, C.; Xiong, J.; Tao, J.; Xu, S.; Zhang, D.; Lin, H.; Chen, Y. Sodium alginate/graphene oxide aerogel with enhanced strength-toughness and its heavy metal adsorption study. *Int. J. Biol. Macromol.* **2016**, *83*, 133–141. [[CrossRef](#)]
140. Syeda, H.I.; Yap, P.-S. A review on three-dimensional cellulose-based aerogels for the removal of heavy metals from water. *Sci. Total Environ.* **2022**, *807*, 150606. [[CrossRef](#)]
141. Fricke, J.; Emmerling, A. Aerogels—Preparation, properties, applications. In *Chemistry, Spectroscopy and Applications of Sol-Gel Glasses*; Reisfeld, R., Jørgensen, C.K., Eds.; Springer: Berlin/Heidelberg, Germany, 1992; pp. 37–87.
142. Jiao, C.; Li, T.; Wang, J.; Wang, H.; Zhang, X.; Han, X.; Du, Z.; Shang, Y.; Chen, Y. Efficient Removal of Dyes from Aqueous Solution by a Porous Sodium Alginate/gelatin/graphene Oxide Triple-network Composite Aerogel. *J. Polym. Environ.* **2020**, *28*, 1492–1502. [[CrossRef](#)]
143. Wang, M.; Wang, Z.; Zhou, X.; Li, S. Efficient Removal of Heavy Metal Ions in Wastewater by Using a Novel Alginate-EDTA Hybrid Aerogel. *Appl. Sci.* **2019**, *9*, 547. [[CrossRef](#)]
144. Hassan, M.; Naidu, R.; Du, J.; Qi, F.; Ahsan, M.A.; Liu, Y. Magnetic responsive mesoporous alginate/ β -cyclodextrin polymer beads enhance selectivity and adsorption of heavy metal ions. *Int. J. Biol. Macromol.* **2022**, *207*, 826–840. [[CrossRef](#)] [[PubMed](#)]
145. Prinz Setter, O.; Segal, E. Halloysite nanotubes—The nano-bio interface. *Nanoscale* **2020**, *12*, 23444–23460. [[CrossRef](#)]
146. Norkus, E. Metal ion complexes with native cyclodextrins. An overview. *J. Incl. Phenom. Macrocycl. Chem.* **2009**, *65*, 237–248. [[CrossRef](#)]
147. Pedroso-Santana, S.; Fleitas-Salazar, N. Iontropic gelation method in the synthesis of nanoparticles/microparticles for biomedical purposes. *Polym. Int.* **2020**, *69*, 443–447. [[CrossRef](#)]
148. Alver, E.; Metin, A.Ü.; Brouers, F. Methylene blue adsorption on magnetic alginate/rice husk bio-composite. *Int. J. Biol. Macromol.* **2020**, *154*, 104–113. [[CrossRef](#)]
149. Shi, T.; Xie, Z.; Zhu, Z.; Shi, W.; Liu, Y.; Liu, M. Highly efficient and selective adsorption of heavy metal ions by hydrazide-modified sodium alginate. *Carbohydr. Polym.* **2022**, *276*, 118797. [[CrossRef](#)]
150. Zhu, R.; Chen, Q.; Zhou, Q.; Xi, Y.; Zhu, J.; He, H. Adsorbents based on montmorillonite for contaminant removal from water: A review. *Appl. Clay Sci.* **2016**, *123*, 239–258. [[CrossRef](#)]
151. Wang, W.; Fan, M.; Ni, J.; Peng, W.; Cao, Y.; Li, H.; Huang, Y.; Fan, G.; Zhao, Y.; Song, S. Efficient dye removal using fixed-bed process based on porous montmorillonite nanosheet/poly(acrylamide-co-acrylic acid)/sodium alginate hydrogel beads. *Appl. Clay Sci.* **2022**, *219*, 106443. [[CrossRef](#)]
152. Sezen, S.; Thakur, V.K.; Ozmen, M.M. Highly Effective Covalently Crosslinked Composite Alginate Cryogels for Cationic Dye Removal. *Gels* **2021**, *7*, 178. [[CrossRef](#)]
153. Isawi, H. Using Zeolite/Polyvinyl alcohol/sodium alginate nanocomposite beads for removal of some heavy metals from wastewater. *Arab. J. Chem.* **2020**, *13*, 5691–5716. [[CrossRef](#)]
154. Parameswaran, B. Sugarcane Bagasse. In *Biotechnology for Agro-Industrial Residues Utilisation: Utilisation of Agro-Residues*; Singh nee' Nigam, P., Pandey, A., Eds.; Springer: Dordrecht, The Netherlands, 2009; pp. 239–252.
155. Fan, S.; Zhou, J.; Zhang, Y.; Feng, Z.; Hu, H.; Huang, Z.; Qin, Y. Preparation of sugarcane bagasse succinate/alginate porous gel beads via a self-assembly strategy: Improving the structural stability and adsorption efficiency for heavy metal ions. *Bioresour. Technol.* **2020**, *306*, 123128. [[CrossRef](#)] [[PubMed](#)]

156. Yadav, M.; Goswami, P.; Paritosh, K.; Kumar, M.; Pareek, N.; Vivekanand, V. Seafood waste: A source for preparation of commercially employable chitin/chitosan materials. *Bioresour. Bioprocess.* **2019**, *6*, 8. [[CrossRef](#)]
157. Hamed, I.; Özogul, F.; Regenstein, J.M. Industrial applications of crustacean by-products (chitin, chitosan, and chito oligosaccharides): A review. *Trends Food Sci. Technol.* **2016**, *48*, 40–50. [[CrossRef](#)]
158. Pakizeh, M.; Moradi, A.; Ghassemi, T. Chemical extraction and modification of chitin and chitosan from shrimp shells. *Eur. Polym. J.* **2021**, *159*, 110709. [[CrossRef](#)]
159. Younes, I.; Rinaudo, M. Chitin and Chitosan Preparation from Marine Sources. Structure, Properties and Applications. *Mar. Drugs* **2015**, *13*, 1133–1174. [[CrossRef](#)]
160. Desbrières, J.; Guibal, E. Chitosan for wastewater treatment. *Polym. Int.* **2018**, *67*, 7–14. [[CrossRef](#)]
161. Gerente, C.; Lee, V.K.C.; Cloirec, P.L.; McKay, G. Application of Chitosan for the Removal of Metals from Wastewaters by Adsorption—Mechanisms and Models Review. *Crit. Rev. Environ. Sci. Technol.* **2007**, *37*, 41–127. [[CrossRef](#)]
162. Zhao, J.; Zou, Z.; Ren, R.; Sui, X.; Mao, Z.; Xu, H.; Zhong, Y.; Zhang, L.; Wang, B. Chitosan adsorbent reinforced with citric acid modified β -cyclodextrin for highly efficient removal of dyes from reactive dyeing effluents. *Eur. Polym. J.* **2018**, *108*, 212–218. [[CrossRef](#)]
163. Usman, M.; Ahmed, A.; Yu, B.; Wang, S.; Shen, Y.; Cong, H. Simultaneous adsorption of heavy metals and organic dyes by β -Cyclodextrin-Chitosan based cross-linked adsorbent. *Carbohydr. Polym.* **2021**, *255*, 117486. [[CrossRef](#)]
164. Karimi-Maleh, H.; Ranjbari, S.; Tanhaei, B.; Ayati, A.; Orooji, Y.; Alizadeh, M.; Karimi, F.; Salmanpour, S.; Rouhi, J.; Sillanpää, M.; et al. Novel 1-butyl-3-methylimidazolium bromide impregnated chitosan hydrogel beads nanostructure as an efficient nanobio-adsorbent for cationic dye removal: Kinetic study. *Environ. Res.* **2021**, *195*, 110809. [[CrossRef](#)] [[PubMed](#)]
165. Fan, S.; Chen, J.; Fan, C.; Chen, G.; Liu, S.; Zhou, H.; Liu, R.; Zhang, Y.; Hu, H.; Huang, Z.; et al. Fabrication of a CO₂-responsive chitosan aerogel as an effective adsorbent for the adsorption and desorption of heavy metal ions. *J. Hazard. Mater.* **2021**, *416*, 126225. [[CrossRef](#)] [[PubMed](#)]
166. Mu, R.; Liu, B.; Chen, X.; Wang, N.; Yang, J. Adsorption of Cu (II) and Co (II) from aqueous solution using lignosulfonate/chitosan adsorbent. *Int. J. Biol. Macromol.* **2020**, *163*, 120–127. [[CrossRef](#)] [[PubMed](#)]
167. Zhang, F.; Wang, B.; Jie, P.; Zhu, J.; Cheng, F. Preparation of chitosan/lignosulfonate for effectively removing Pb (II) in water. *Polymer* **2021**, *228*, 123878. [[CrossRef](#)]
168. Yadav, V.; Kumar, A.; Bilal, M.; Nguyen, T.A.; Iqbal, H.M.N. Chapter 12—Lignin removal from pulp and paper industry waste streams and its application. In *Nanotechnology in Paper and Wood Engineering*; Bhat, R., Kumar, A., Nguyen, T.A., Sharma, S., Eds.; Elsevier: Amsterdam, The Netherlands, 2022; pp. 265–283.
169. Ralph, J.; Lapiere, C.; Boerjan, W. Lignin structure and its engineering. *Curr. Opin. Biotechnol.* **2019**, *56*, 240–249. [[CrossRef](#)] [[PubMed](#)]
170. Ponnusamy, V.K.; Nguyen, D.D.; Dharmaraja, J.; Shobana, S.; Banu, J.R.; Saratale, R.G.; Chang, S.W.; Kumar, G. A review on lignin structure, pretreatments, fermentation reactions and biorefinery potential. *Bioresour. Technol.* **2019**, *271*, 462–472. [[CrossRef](#)]
171. Zhao, X.; Wang, X.; Lou, T. Preparation of fibrous chitosan/sodium alginate composite foams for the adsorption of cationic and anionic dyes. *J. Hazard. Mater.* **2021**, *403*, 124054. [[CrossRef](#)]
172. Tang, S.; Yang, J.; Lin, L.; Peng, K.; Chen, Y.; Jin, S.; Yao, W. Construction of physically crosslinked chitosan/sodium alginate/calcium ion double-network hydrogel and its application to heavy metal ions removal. *Chem. Eng. J.* **2020**, *393*, 124728. [[CrossRef](#)]
173. Ablouh, E.-H.; Hanani, Z.; Eladlani, N.; Rhazi, M.; Taourirte, M. Chitosan microspheres/sodium alginate hybrid beads: An efficient green adsorbent for heavy metals removal from aqueous solutions. *Sustain. Environ. Res.* **2019**, *29*, 5. [[CrossRef](#)]
174. Khapre, M.A.; Pandey, S.; Jugade, R.M. Glutaraldehyde-cross-linked chitosan-alginate composite for organic dyes removal from aqueous solutions. *Int. J. Biol. Macromol.* **2021**, *190*, 862–875. [[CrossRef](#)]
175. Hamza, M.F.; Hamad, N.A.; Hamad, D.M.; Khalafalla, M.S.; Abdel-Rahman, A.A.-H.; Zeid, I.F.; Wei, Y.; Hessien, M.M.; Fouda, A.; Salem, W.M. Synthesis of Eco-Friendly Biopolymer, Alginate-Chitosan Composite to Adsorb the Heavy Metals, Cd(II) and Pb(II) from Contaminated Effluents. *Materials* **2021**, *14*, 2189. [[CrossRef](#)] [[PubMed](#)]
176. Carvalho, A.J.F. Chapter 15—Starch: Major Sources, Properties and Applications as Thermoplastic Materials. In *Monomers, Polymers and Composites from Renewable Resources*; Belgacem, M.N., Gandini, A., Eds.; Elsevier: Amsterdam, The Netherlands, 2008; pp. 321–342.
177. Vandenbossche, M.; Jimenez, M.; Casetta, M.; Traisnel, M. Remediation of Heavy Metals by Biomolecules: A Review. *Crit. Rev. Environ. Sci. Technol.* **2015**, *45*, 1644–1704. [[CrossRef](#)]
178. Robyt, J.F. Starch: Structure, Properties, Chemistry, and Enzymology. In *Glycoscience: Chemistry and Chemical Biology*; Fraser-Reid, B.O., Tatsuta, K., Thiem, J., Eds.; Springer: Berlin/Heidelberg, Germany, 2008; pp. 1437–1472.
179. Kringel, D.H.; Dias, A.R.G.; Zavareze, E.D.R.; Gandra, E.A. Fruit Wastes as Promising Sources of Starch: Extraction, Properties, and Applications. *Starch* **2020**, *72*, 1900200. [[CrossRef](#)]

180. Awokoya, K.N.; Oninla, V.O.; Bello, D.J. Synthesis of oxidized *Dioscorea dumentorum* starch nanoparticles for the adsorption of lead(II) and cadmium(II) ions from wastewater. *Environ. Nanotechnol. Monit. Manag.* **2021**, *15*, 100440. [[CrossRef](#)]
181. Abd El-Ghany, N.A.; Elella, M.H.A.; Abdallah, H.M.; Mostafa, M.S.; Samy, M. Recent Advances in Various Starch Formulation for Wastewater Purification via Adsorption Technique: A Review. *J. Polym. Environ.* **2023**, *31*, 2792–2825. [[CrossRef](#)]
182. Haroon, M.; Wang, L.; Yu, H.; Abbasi, N.M.; Zain-ul-Abdin; Saleem, M.; Khan, R.U.; Ullah, R.S.; Chen, Q.; Wu, J. Chemical modification of starch and its application as an adsorbent material. *RSC Adv.* **2016**, *6*, 78264–78285. [[CrossRef](#)]
183. Guo, L.; Li, G.; Liu, J.; Meng, Y.; Tang, Y. Adsorptive decolorization of methylene blue by crosslinked porous starch. *Carbohydr. Polym.* **2013**, *93*, 374–379. [[CrossRef](#)]
184. Alvarado, N.; Abarca, R.L.; Urdaneta, J.; Romero, J.; Galotto, M.J.; Guarda, A. Cassava starch: Structural modification for development of a bio-adsorber for aqueous pollutants. Characterization and adsorption studies on methylene blue. *Polym. Bull.* **2021**, *78*, 1087–1107. [[CrossRef](#)]
185. Soto, D.; Urdaneta, J.; Pernía, K.; León, O.; Muñoz-Bonilla, A.; Fernández-García, M. Removal of heavy metal ions in water by starch esters. *Starch* **2016**, *68*, 37–46. [[CrossRef](#)]
186. Soto, D.; Urdaneta, J.; Pernía, K.; León, O.; Muñoz-Bonilla, A.; Fernández-García, M. Heavy metal (Cd²⁺, Ni²⁺, Pb²⁺ and Ni²⁺) adsorption in aqueous solutions by oxidized starches. *Polym. Adv. Technol.* **2015**, *26*, 147–152. [[CrossRef](#)]
187. Sancey, B.; Trunfio, G.; Charles, J.; Minary, J.-F.; Gavaille, S.; Badot, P.-M.; Crini, G. Heavy metal removal from industrial effluents by sorption on cross-linked starch: Chemical study and impact on water toxicity. *J. Environ. Manag.* **2011**, *92*, 765–772. [[CrossRef](#)]
188. Zheng, Y.; Hua, S.; Wang, A. Adsorption behavior of Cu²⁺ from aqueous solutions onto starch-g-poly(acrylic acid)/sodium humate hydrogels. *Desalination* **2010**, *263*, 170–175. [[CrossRef](#)]
189. Chaudhari, S.; Tare, V. Analysis and evaluation of heavy metal uptake and release by insoluble starch xanthate in aqueous environment. *Water Sci. Technol.* **1996**, *34*, 161–168. [[CrossRef](#)]
190. Zubair, M.; Jarrah, N.; Ihsanullah; Khalid, A.; Manzar, M.S.; Kazeem, T.S.; Al-Harthi, M.A. Starch-NiFe-layered double hydroxide composites: Efficient removal of methyl orange from aqueous phase. *J. Mol. Liq.* **2018**, *249*, 254–264. [[CrossRef](#)]
191. Tao, X.; Liu, D.; Cong, W.; Huang, L. Controllable synthesis of starch-modified ZnMgAl-LDHs for adsorption property improvement. *Appl. Surf. Sci.* **2018**, *457*, 572–579. [[CrossRef](#)]
192. Liu, J.; Yue, X.; Lu, X.; Guo, Y. Uptake Fluoride from Water by Starch Stabilized Layered Double Hydroxides. *Water* **2018**, *10*, 745. [[CrossRef](#)]
193. Hao, L.; Liu, M.; Wang, N.; Li, G. A critical review on arsenic removal from water using iron-based adsorbents. *RSC Adv.* **2018**, *8*, 39545–39560. [[CrossRef](#)]
194. Xu, F.; Chen, H.; Dai, Y.; Wu, S.; Tang, X. Arsenic adsorption and removal by a new starch stabilized ferromanganese binary oxide in water. *J. Environ. Manag.* **2019**, *245*, 160–167. [[CrossRef](#)]
195. Siddiqui, S.I.; Singh, P.N.; Tara, N.; Pal, S.; Chaudhry, S.A.; Sinha, I. Arsenic removal from water by starch functionalized maghemite nano-adsorbents: Thermodynamics and kinetics investigations. *Colloids Interface Sci. Commun.* **2020**, *36*, 100263. [[CrossRef](#)]
196. Robinson, M.R.; Coustel, R.; Abdelmoula, M.; Mallet, M. As (V) and As (III) sequestration by starch functionalized magnetite nanoparticles: Influence of the synthesis route onto the trapping efficiency. *Sci. Technol. Adv. Mater.* **2020**, *21*, 524–539. [[CrossRef](#)]
197. Ma, X.; Liu, X.; Anderson, D.P.; Chang, P.R. Modification of porous starch for the adsorption of heavy metal ions from aqueous solution. *Food Chem.* **2015**, *181*, 133–139. [[CrossRef](#)] [[PubMed](#)]
198. Liu, Q.; Li, F.; Lu, H.; Li, M.; Liu, J.; Zhang, S.; Sun, Q.; Xiong, L. Enhanced dispersion stability and heavy metal ion adsorption capability of oxidized starch nanoparticles. *Food Chem.* **2018**, *242*, 256–263. [[CrossRef](#)] [[PubMed](#)]
199. Chen, Q.-J.; Zheng, X.-M.; Zhou, L.-L.; Zhang, Y.-F. Adsorption of Cu (II) and Methylene Blue by Succinylated Starch Nanocrystals. *Starch* **2019**, *71*, 1800266. [[CrossRef](#)]
200. Hashem, A.; Ahmad, F.; Fahad, R. Application of some starch hydrogels for the removal of mercury (II) ions from aqueous solutions. *Adsorpt. Sci. Technol.* **2008**, *26*, 563–579. [[CrossRef](#)]
201. Aniagor, C.O.; Afifi, M.A.; Hashem, A. Rapid and efficient uptake of aqueous lead pollutant using starch-based superabsorbent hydrogel. *Polym. Bull.* **2022**, *79*, 6373–6388. [[CrossRef](#)]
202. Haroon, M.; Wang, L.; Yu, H.; Ullah, R.S.; Zain-ul-Abdin; Khan, R.U.; Chen, Q.; Liu, J. Synthesis of carboxymethyl starch-g-polyvinylpyrrolidones and their properties for the adsorption of Rhodamine 6G and ammonia. *Carbohydr. Polym.* **2018**, *186*, 150–158. [[CrossRef](#)]
203. Ma, K.; Zhao, L.; Jiang, Z.; Huang, Y.; Sun, X. Adsorption characteristics of Cr (III) onto starch-graft-poly(acrylic acid)/organo-modified zeolite 4A composite: A novel path to the adsorption mechanisms. *Polym. Compos.* **2018**, *39*, 1223–1233. [[CrossRef](#)]
204. Chen, L.; Zhu, Y.; Cui, Y.; Dai, R.; Shan, Z.; Chen, H. Fabrication of starch-based high-performance adsorptive hydrogels using a novel effective pretreatment and adsorption for cationic methylene blue dye: Behavior and mechanism. *Chem. Eng. J.* **2021**, *405*, 126953. [[CrossRef](#)]

205. Shoaib, A.G.M.; Sikaily, A.E.; Ragab, S.; Masoud, M.S.; Ramadan, M.S.; El Nemr, A. Starch-grafted-poly(acrylic acid)/Pterocladia capillacea-derived activated carbon composite for removal of methylene blue dye from water. *Biomass Convers. Biorefinery* **2022**. [[CrossRef](#)]
206. Zhang, H.; Wang, P.; Zhang, Y.; Cheng, B.; Zhu, R.; Li, F. Synthesis of a novel arginine-modified starch resin and its adsorption of dye wastewater. *RSC Adv.* **2020**, *10*, 41251–41263. [[CrossRef](#)]
207. Jiang, H.; Yang, Y.; Lin, Z.; Zhao, B.; Wang, J.; Xie, J.; Zhang, A. Preparation of a novel bio-adsorbent of sodium alginate grafted polyacrylamide/graphene oxide hydrogel for the adsorption of heavy metal ion. *Sci. Total Environ.* **2020**, *744*, 140653. [[CrossRef](#)] [[PubMed](#)]

Disclaimer/Publisher's Note: The statements, opinions and data contained in all publications are solely those of the individual author(s) and contributor(s) and not of MDPI and/or the editor(s). MDPI and/or the editor(s) disclaim responsibility for any injury to people or property resulting from any ideas, methods, instructions or products referred to in the content.